***Large-scale atmospheric response to Mediterranean SST anomalies: impacts on the Atlantic climate variability and applications for seasonal forecasting***

This project was proposed for the ESF-MedCLIVAR grants to support the scientific visit of Mr. Javier García Serrano, PhD student in the Climate Variability Group at the Universidad Complutense de Madrid (Spain), for spenting 17 weeks at the Met Office-Hadley Centre (United Kingdom). The exchange-visit was joined in the Seasonal Forecasting Group (led by Dr. Alberto Arribas) which is part of the Modelling Climate Variability research area (led by Dr. Adam Scaife).

The visit was framed in one of the five main themes of the ESF-MedCLIVAR Programme: 'Connections between Mediterranean and global climate variability'. The proposed study was also following some of the key CLIVAR research areas, concretely: 'Interannual variability of the African climate system', 'Tropical Atlantic Variability' and 'Regional effects of Climate Change'.

## Purpose of the visit

The aim of this exchange grant is to analyse and give evidences of a large-scale atmospheric response to summer Mediterranean sea surface temperature (SST) anomalies with the advice of Adam Scaife's group (Modelling Climate Variability), Richard Graham's group (Climate Applications Development) and Chris Folland's group (Climate Research), who are wellknown by their regional and global teleconnections studies. On the other hand, the Met Office-Hadley Centre is one of the most prestigious meteorological services in seasonal forecast, thereby the results derived from this project could contribute substantially to the improvement of the seasonal prediction system.

The work is based on a preliminary study presented at 2$^{nd}$ ESF-MedCLIVAR Workshop (García-Serrano et al. 2007; enclosed in the Appendix) and constitutes the next step in a new research line of our group (Polo et al. 2008). On the one hand, and regarding the latter paper, Polo et al. shows how the Mediterranean Sea appears to have an isolated active role in the West African Monsoon (WAM) rainfall variability and, concretely, in the Sahelian precipitation anomalies. The results are found for the recent decades, after the so-called *Climate Shift* (e.g. Cane et al. 1997, Seidel et al. 2008), a period for which the Sahelian seasonal rainfall has experimented a longer drought, one of the strongest interdecadal signal on the climate in the 20$^{th}$ century (e.g. Giannini et al. 2003). On the other hand, and besides the impact of the Mediterranean SST on the WAM variability during recent decades (Polo et al. 2008), García-Serrano et al. (2007) points to a possible large-scale atmospheric response to summer Mediterranean SSTs. Such a relevant feature was formulated on the basis of a recent encouraging work by Li (2006), in which the author hypothesizes and demonstrates, for the first time, that winter Mediterranean SST anomalies could force a global atmospheric pattern.
It is worthy to study the impact on the WAM-Sahel rainfall of this large-scale atmospheric response to Mediterranean SST anomalies because recent studies have shown controversial results when analysing the key role in the long-term drying suffered in the region. The debate is mainly whether the WAM system responds to a thermal forcing (e.g. Giannini et al. 2003) or anthropogenic land-surface modifications (e.g. Held et al. 2005). On the subject, Hoerling et al. (2006) report that a multi-model ensemble forced with 20th century anthropogenic emissions reproduces the long-term variations of Indian Ocean and (less accurately) Atlantic Ocean SST, but fails to

reproduce the magnitude of the observed 1950-1980 Sahel drying. It is also important to notice that usually many aspects of Sahel rainfall variability have been linked to SSTs solely over the Indo-Pacific and Atlantic basins (e.g. Held et al. 2005, Biasutti and Giannini 2006), overlooking the potential role of the Mediterranean Sea. Conversely, a number of works have found significant relationships with Mediterranean anomalies (e.g. Raicich et al. 2003, Rowell 2003, Fontaine et al. 2003, Jung et al. 2006, Fontaine et al. 2008). However, these studies have had a marked regional point of view in the connection. On the contrary, this work explores the Mediterranean SST-Sahel rainfall relation with the aim to characterize the large-scale features in the covariability.

Li (2006) made an idealized cooling-experiment of 2K for the Mediterranean to find the above-mention results. In the present work, observations (ERA40), experiments with an AGCM (UCLA model) and two coupled OAGCM (HadGEM-family models) are investigated to test whether the mechanism found in the model study of Li (2006) can be identified also in the real world. In particular, and following the relevant outcomes by Branstator (2002) concerning the circumglobal teleconnections, Li (2006) hypothetised and demonstrated the ability of the Mediterranean SST anomalies in forcing a global-waveguided atmospheric response. Two remarkable remote features were shown: the deepening of the Aleutian Low in the North Pacific and the weakening of the Icelandic Low in the North Atlantic. Also, another two recent works support the importance of the Mediterranean basin, particularly the convergence over the Sea, in favouring the establishment of a hemispheric pattern which resembles the Artic Oscillation (AO) rather than the North Atlantic Oscillation (NAO) (Kodera and Kuroda 2003, Watanabe 2004). Diagnoses using a linear barotropic model, shown by Watanabe (2004), indicate the downstream propagation of Rossby waves trapped on the North African-Asian jet waveguide (hereafter, NAA jet; Hoskins and Ambrizzi 1993) effectively excited by the anomalous upper-level convergence over the Mediterranean.

Very relevant results have been found following the above hypotheses. The consequences derived of the main objective concerns **global teleconnections** and related climate impacts. In this way, the project highlights the **pivotal role of the Mediterranean Sea** not only as local forcing but also **as a large-scale predictor**. The associated phenomena include the influence on the midlatitudes-subtropical basic state (North African-Asian jet), the WAM monsoonal rainfall (Sudan-Sahel region) and the climate variability in the western North Pacific basin (Pacific Decadal Oscillation). All above studies focused the analysis on boreal wintertime; therefore, this project, regarding the impacts in **summertime**, presents a work that has not been documented yet. In addition, as shown by Xoplaki et al. (2003a-b), a great amount of interannual air temperature variance is associated with the same Mediterranean warming (eastern basin) analyzed in the project: first local EOF-CCA mode (2003a's paper) and second basin-wide EOF-CCA mode (2003b's paper). Hence, the results presented here are also of great interest for the **Mediterranean climate variability itself**.

## Description of the work carried out during the visit

During the 17 weeks of the visit, I focused my work on performing numerical experiments and analysing observations and simulations with the aim of supporting the initial hypotheses.
Nevertheless, during the first weeks I tried to learn the basic commands to manage, as well as I could, in the new operative system, the Met Office's system: RedHat distribution of Linux (I used to work in Windows at UCM). In the same way, I also learnt the basic commands for the 'command window' of the Met Office's software for

computation (PV-Wave; I used to work with GrADS and Matlab) as well as the digital language of its scripts (.pro, of processor) for manipulating the particular Met Office's data (pp-fields). In addition, I had to learn some UKMO libraries (for PV-Wave) to move our binary and netcdf datasets on pp-field format. In particular, the pp-fields have similar characteristics that netcdf format but with a particular digital weight and much more information in the header. The pp-fields as outputs of the coupled Ocean-Atmosphere GCM (OAGCM) models from HadGEMs family have a very high spatial resolution. Concretely, datasets I have used present 1.875-lon by 1.25-lat (192x144) grid points for atmospheric variables, and higher resolution for oceanic data (360x216): regular-1degree by longitude and roughly irregular-1degree by latitude with 14 levels in depth. During my visit I have worked with two old-versions (currently, it is developing the third version) of the HadGEM-family, particularly with HadGEM-1 (hereafter, HadGEM1) and the simplified Ocean-Atmosphere HadGEM-2, the OA-HadGEM-2 (hereafter, HadGEM2).

At the same time, I completed the bibliography related to this project, as read them. Because the secondary objectives were changing in the course of time, once the hypothesis of global response to Mediterranean SST was established, the bibliography for each issue would request a continue actualization. In general, throughout the exchange-visit, I have compiled a very interesting list of articles not only concerning the Mediterranean climate variability but also regarding dynamics of the teleconnections found, mechanisms involved, climate impacts and potentially-influenced variability modes. Framing on each subject (see References for complete citations):

- Atmospheric circulation associated with the Mediterranean
  Fontaine et al. (2008); Haarsma et al. (2008); Jung et al. (2006); Michaelides (1983); Raicich et al. (2003); Rowell (2003); Xoplaki et al. (2003a); Xoplaki et al. (2003b)

- Wave-mean flow interaction and teleconnection dynamics
  Branstator (2002); Chang et al. (2002); Ding and Wang (2005); Hoskins et al. (1983); Kodera and Kuroda (2003); Rodwell and Hoskins (1996); Trenberth (1986); Watanabe (2004)

- West African Monsoon system
  Biasutti and Giannini (2006); Cook (1999); Fontaine et al. (2003); Giannini et al. (2003); Grist et al. (2002); Held et al. (2005); Hoerling et al. (2006); Hsieh and Cook (2005); Joly et al (2007); Mekonnen et al. (2006); Moron et al. (2004); Nicholson (2008); Nicholson and Grist (2001); Nicholson et al. (2007); Nicholson et al. (2008)

- Pacific Decadal Oscillation
  Barnett et al. (1999); Bond and Harrison (2000); Gershunov and Barnett (1998); Trenberth and Hurrell (1994); Zhang et al. (1997)

Besides the above mentioned co-lateral tasks, the main blocks of work of my visit are :

## 1. Development of a software to calculate the Rossby wave sources

This work was done during the first 10 weeks of the visit, parallel to the block 3 as a part of the analysis. The script that I developed makes up a current diagnostic in the post-processing of the HadGEMs-outputs as consequence of my exchange-visit.
In this way, the necessary software to calculate two basic 2D-potentials of the flow was performed: the streamfunction (rotational part of the flow) and velocity potential

(divergent part of the flow), from the horizontal wind (u,v). This problem has been widely described in the concerning literature (Sardeshmukh and Hoskins 1987, Kundu 1990), and it is commonly named PSI-problem and CHI-problem (both, Poisson equations), respectively:

$$\text{PSI-problem:} \quad vort = \nabla^2 \psi \qquad\qquad \text{CHI-problem:} \quad div = \nabla^2 \chi$$

where *vort* and *div* represent the third component of the vorticity (the relative vorticity) and the horizontal divergence of the flow; and $\psi$ and $\chi$ are indicating the streamfunction and the velocity potential; while $\nabla^2$ identifies the Laplacian operator.
Subsequently, once the 2D-potentials are calculated we are in the position to obtain the derived-components of the flow (the rotational and divergent winds) as well as the Rossby wave sources (RWS), an important diagnostic for analysing both tropical and extratropical teleconnections (Sardeshmukh and Hoskins 1988, Qin and Robinson 1993, Watanabe 2004). For these purposes I also implemented a "finite-differences schema" for regular and horizontal grids (ERA40 and HadGEMs): checking those results provided by UKMO-PV Wave routines (pp_grad), and in order to move the developed scripts on Matlab code (afterwards at UCM).

The first approach to resolve the inversion of the Poisson equations, detailed above, was using the classical recurrence equation called "the four-neighbors schema" applied on the horizontal plane with Drichlet conditions (Fig. 1).

$$\zeta_{i,j} = \left(\psi_{i+1,j} + \psi_{i-1,j} - 2\psi_{i,j}\right)/\left(\Delta y\right)^2 \quad + \quad \left(\psi_{i,j+1} + \psi_{i,j-1} - 2\psi_{i,j}\right)/\left(R\cos\varphi_{i,j} \cdot \Delta\lambda\right)^2$$

A great number of white-pages were used to obtain the correct matrix for the Poisson's inversion (with the correct order of the elements for the latitude-longitude order of the data). As it is easily observable in Fig. 1, the results propagate the edge-effects so far from the domain limits so this technique claimed to be improved. For this reason, in a second approach the previous inversion matrix was moved with periodic conditions in longitude, but the resulting 2D flow-potentials remained showing some problems with conditions in the polar caps (not shown). A final approach was to translate the original problem into the time-frequency domain for resolving the problem via spherical harmonics (Fig. 2; Sardeshmukh and Hoskins 1987).

An example of the PV-Wave scripts generated is attached in the Appendix. That script, named 'RWS_diagnostic.pro', resolve the PSI and CHI problems calling, respectively, the external 'pp_strmfn' and 'pp_velpot' scripts; and calculate both the rotational-divergent components of the wind and the different RWS terms calling the subroutine 'calc_dyn_fields'. Below are shown the streamfunction, rotational wind and tropical-RWS (Fig. 3-top); and the velocity potential, divergent wind and extratropical-RWS (Fig. 3-bottom) for the ERA40 winter climatology at 200hPa.
The dominant anomalous RWS terms are the anomalous tropical-RWS (TRWS), associated with the advection of the climatological vorticity, and the anomalous extratropical-RWS (ERWS), associated with regions of divergence/convergence anomaly (Qin and Robinson 1993):

$$TRWS = -v'_{\chi} \cdot \nabla\left(\overline{\zeta} + f\right) \qquad\qquad ERWS = -\left(\overline{\zeta} + f\right)\nabla \cdot v'_{\chi}$$

where $v'_{\chi}$ is the anomalous divergent wind, $\overline{\zeta}$ is the climatological relative vorticity and $f$ the planetary vorticity (Coriolis parameter).

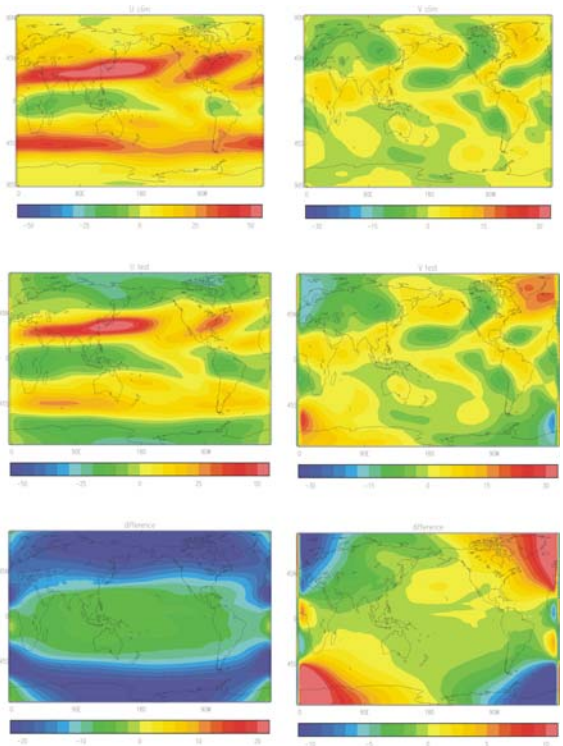

Figure 1. Outcomes after resolving both PSI and CHI problems using Dirichlet boundary conditions. [top] DJF climatological average for zonal (left) and meridional (right) wind at 200hPa from HadGEM2. [middle] Estimation for horizontal 200hPa-wind climatology by adding rotational and divergent parts for each component of the flow; test for zonal (left) and meridional (right) components. [bottom] Difference between original (input, top) and estimated (output, middle) components of the wind climatology at 200hPa.

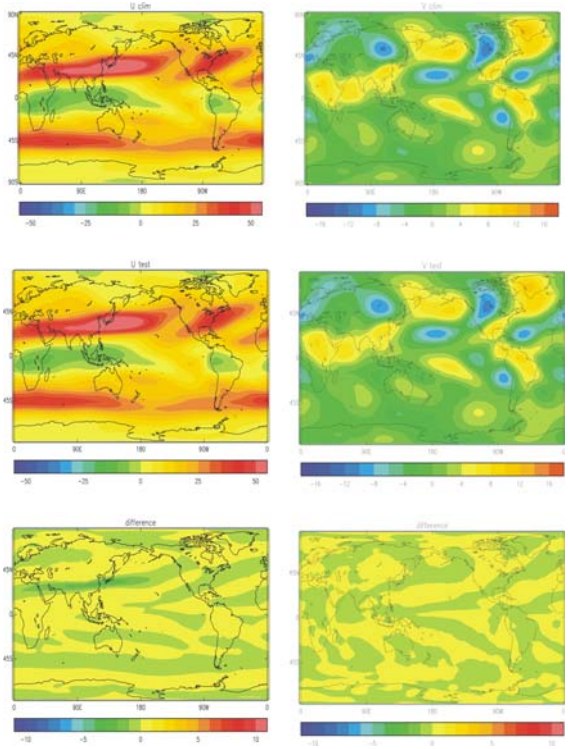

Figure 2. As Figure 1, but after resolving both PSI and CHI problems using spherical harmonics in the time-frequency domain.

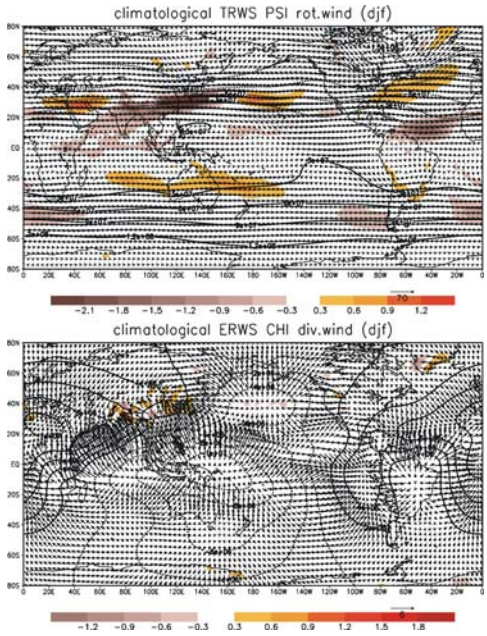


Figure 3. [top] Streamfunction (contours, ci=3 $10^7$ $m^2/s$), rotational wind (arrows) and TRWS (shaded, ci=1 $10^{-10}$ $s^{-2}$); and [bottom] velocity potential (contours, ci=2 $10^6$ $m^2/s$), divergent wind (arrows) and ERWS (shaded, ci=1 $10^{-9}$ $s^{-2}$) for the ERA40 DJF climatology at 200hPa.

## 2. Performance of sensitivity experiments with the UCLA-AGCM

During the first two months of visit I performed a sensitivity experiment for the Mediterranean SST-pattern.
The methodology, which is going to be described below, was discussed and analysed with the Met Office advisors who agreed in the novelty of the simulations that were remotely run, from UK, on the UCM computers. This sensitivity experiment was performed using the UCLA-AGCM model (Mechoso et al. 2000); and it was based on the observational Mediterranean-WAM EMCA mode described in Polo et al. (2008).

This EMCA covariability mode has been found in a recent paper by our group (Polo et al. 2008). The boundary condition used in this sensitivity experiment is based on the expansion coefficient (time series) of the first time-evolving mode between Mediterranean SST (from FMAM to SOND) and JJAS-summer WAM rainfall (also in García-Serrano et al. 2007). This methodology is an extension of the classical Maximum Covariance Analysis (MCA or SVD; Bretherton et al. 1992) by introducing more than one time-lag in one of the field-arrays; with the aim of isolating in the same mode the whole sequence of significant covariant SST patterns in relation to the JJAS anomalous WAM precipitation. In this way, a whole picture of the evolution of the Mediterranean SST from early-spring (FMAM) to late-autumn (SOND) is obtained.

We have used this kind of statistical methodology with the aim of taking into account the intrannual evolution of the interannual variability SST-mode. Thus, EMCA method highlights the seasonal dependence of the internannual modes obtained. In contrast, previous works lack in taking into account the month-to-month evolution of these modes, maximizing covariability independently of the other adjacent seasons and presuming the persistence of the anomalies as function of time (e.g. Czaja and Frankignoul 2002, Frankignoul and Kestenare 2005, Ding and Wang 2005).

Although the Mediterranean sensitivity experiment has been completed, the corresponding outputs have not been analyzed yet.

## 3. Study of atmospheric circulation related to the Mediterranean-WAM link

Most of the work done during my visit, coinciding with the main purpose, was focused on investigating the physical mechanisms involved in the summer teleconnections related to the leading ECMA Mediterranean mode. This large-scale response to Mediterranean SST anomalies was analyzed using observations, two OAGCM models (HadGEMs) and one AGCM model (UCLA). The main results related to this third block are described next.

# RESULTS

## *Observations*

### Description of the Mediterranean mode

As commented above, Polo et al. (2008) have recently found, by applying EMCA, a statistical relation implying an active role of the summer Mediterranean SST onto the WAM variability. In that paper, the EMCA methodology was developed and implemented. The authors use EMCA in order to show the whole picture of the Mediterranean SST pattern evolution in relation to the summer (JJAS) WAM-rainfall with a realistic persistence feature from boreal early spring (FMAM) to late autumn (SOND). Complementary to this, EMCA gives the opportunity of increasing the number of time series in the analysis, having as many time series per point as time lags used, and assessing, in this way, the statistically significance of the results.

Fig. 4 represents the leading EMCA mode, which is the starting point for this study, in order to investigate the underlying dynamics and get new insights in the relationship between Mediterranean SST anomalies and the global climate variability.

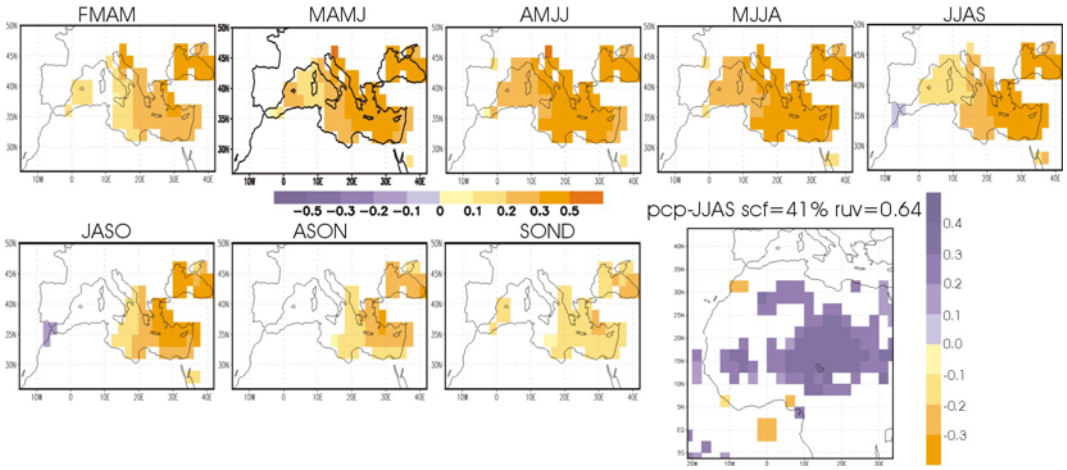


Figure 4. Homogeneous SST (ºC) regression maps for the sequence from early-spring (FMAM) to late-autumn (SOND) obtained from the EMCA analysis. Heterogeneous regression map of the WAM rainfall (JJAS; std anomalies) onto the leading EMCA-SST expansion coefficient. Only 98% statistically significant areas (evaluated with a *t*-test) are plotted. [as Polo et al. 2008]

This mode is related to persistent positive SST anomalies that peak in MJJA. Concretely, EMCA result shows positive Med SST anomalies confined over the eastern part of the basin, associated with higher than normal WAM rainfall over the Sahel, in particular over the region 15N-25N/5E-30E. This EMCA mode explains more than 40%

of the square covariance fraction (scf) and it is a very robust mode, as can be seen after applying 100 Monte Carlo analyses (Fig. 5-bottom).

Also, the correlation of the precipitation expansion coefficient (Fig. 5-top, solid) is statistically significant with the global EMCA SST expansion coefficient (ruv; Fig. 5-top, bars) and the first WAM rainfall EOF (Sahelian mode; Polo et al. 2008): 0.64 and 0.96 respectively. These correlations indicate that the leading EMCA-based WAM pattern, related to the Mediterranean SST, is also the leading WA monsoon-precipitation mode.

Fig. 5 represents the expansion coefficient derived from EMCA for the summer time-varying predictor (Med-SST; bars) and predictand (Sahel-WAM rainfall; solid line). It is apparent the strong decadal signal in the Med-SST time series, according to Xoplaki et al. (2003a-b) in relation to the higher values in the eastern Mediterranean basin. It is also important to notice the covariability between both expansion coefficients, pointing to a stronger relation between the Sahelian rainfall variability and the Mediterranean SST variability for the period 1979-2001 (time-period used here). Even so, the regression of the EMCA-SST expansion coefficient onto the global SST anomalies (see below) reveals that the EMCA-Med mode is associated with central equatorial Pacific SST, rather than central-eastern equatorial Pacific. In fact, the correlation with Niño3.4 is roughly 0.2/0.3 in all time-lags, suggesting that Pacific SST anomalies are not related to a canonical ENSO event. In addition, significant correlations are found between Pacific Decadal Oscillation (PDO) index and the EMCA-Mediterranean mode (discussed below).

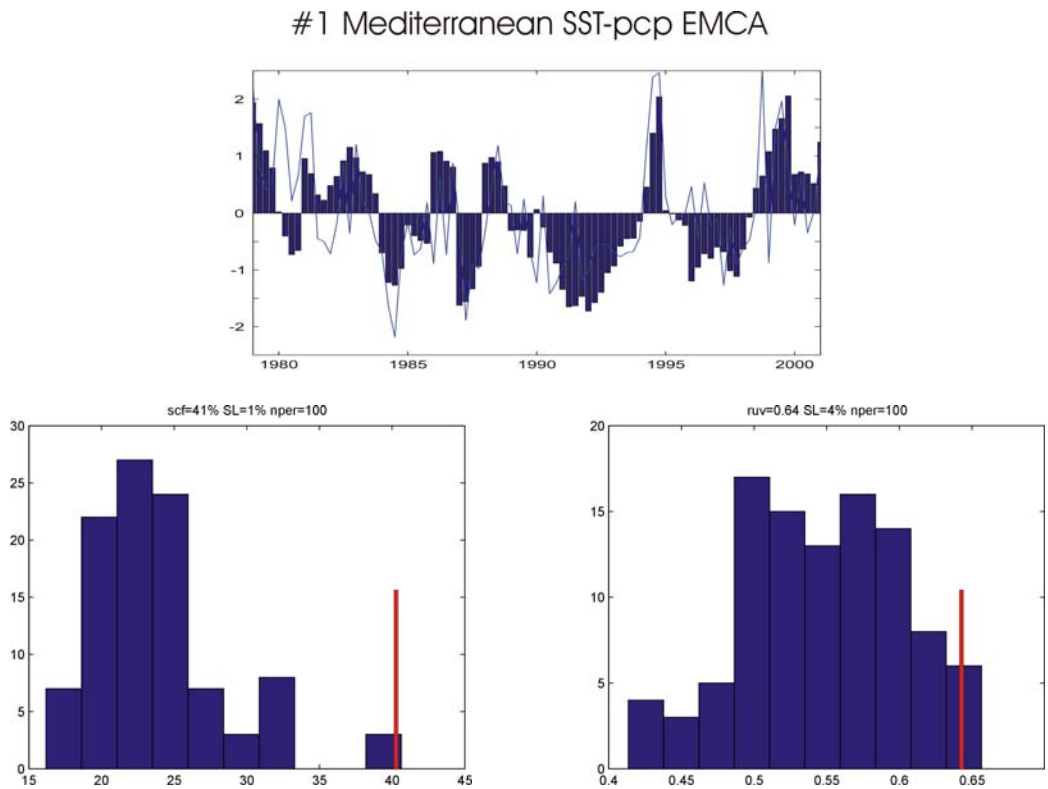


Figure 5. [top] The expansion coefficients corresponding to the leading EMCA mode between Mediterranean SST (NOAA Extended Reconstructed dataset, Smith and Reynolds 2003; bars) and CMAP precipitation (Xie and Arkin 1997; solid line) for the 1979-2001. [bottom] The probability density functions of the *scf* and *ruv* from 100 times Montecarlo test (histogram) is compared with the original EMCA *scf* and *ruv* scores (red line) to show its significance level (SL; indicated in the title)

Fig. 6 represents the seasonal dependence of the EMCA-Med SST expansion coefficients in relation to the Sahelian mode. On the one hand, the global SST expansion coefficient is obtained by using the whole eigenvector (all lags included) of the covariance matrix and, thus, capturing the complete time-evolving pattern. Hence, the global EMCA-SST is adopted for regressing the EMCA information on different variables/fields (Polo et al. 2008, García-Serrano et al. 2008). On the other hand, the individual SST expansion coefficients are calculated for each SST lag. As expected, it is apparent that the correlation between the Sahelian mode and the global EMCA-SST is comparatively maximum; less than the correlation coefficient using the individual EMCA-expansion coefficients (remember, ruv=0.64).

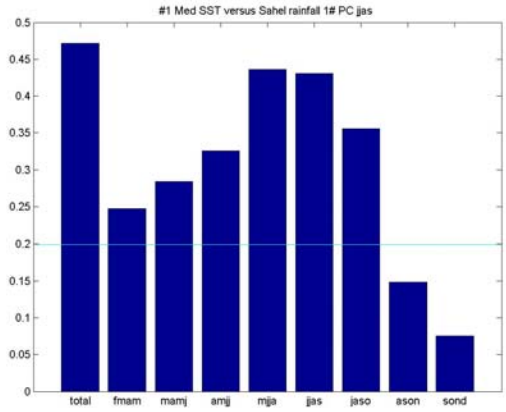


Figure 6. Correlation coefficient between the leading WAM rainfall, the Sahelian mode (Polo et al. 2008), and every SST expansion coefficient obtained from the EMCA-Med; the score associted with the global EMCA-SST time series is indicated in the first column. The horizontal blue line denotes the corresponding Student's *t*-test threshold for the statistical significance.

From FMAM to AMJJ, the correlation it is low although with significant scores; in MJJA, the correlation is maximum, persisting in JJAS and yielding high values up to JASO; while during ASON and SOND the correlation fails the Student's *t*-test. At this moment, it is worthy to note that, added to JJAS (contemporary lag to WAM rainfall), above correlation coefficients suggest either a potential predictability skill (in the case of MJJA) or physical relationship between Med-SST anomalies and Sahel precipitation (for the higher scores-related lags). For that reason, hereafter the analysis is mainly focused on one lag backward and one lag forward to JJAS; that is, MJJA-JJAS-JASO EMCA time-sequences .

**Atmospheric global response to the Mediterranean mode**

In order to find more insights about the anomalous circulation associated to this mode, Fig. 7 shows the regression maps of the streamfunction and rotational wind at 200hPa onto the EMCA-SST expansion coefficient. As indicated above, García-Serrano et al. (2007) proposed a mechanism for explaining the Med-WAM connection. In that work, the streamfunction anomalies from MJJA to JASO show a Med-related upper-tropospheric anomalous anticyclone extending on the adjacent region to the south. This spatial structure closely resemble the mid-upper tropospheric pattern found by Xoplaki et al. (2003a-b) over the Euro-Mediterranean area associated with the eastern-SST anomalies mode.

Since WAM precipitation has a strong component of interannual variability due to the Tropical easterly jet (TEJ; at upper-troposphere) anomalous state (Moron et al. 2004), the suggested mechanism indicates a strengthening of the TEJ, which, together with

the climatological northward displacement of the ITCZ, enhances the Sahelian rainfall, following Nicholson and Grist (2001). This interpreation has changed during the recent study, suggesting a large-scale mechanism which involves perturbations in the Hadley cell instead of perturbations in the TEJ, finally not found (discussed below).
In any case, this finding is partially in agreement with Raicich et al. (2003), because it also implies a circulation change in the Mediterranean surrounding region; although their result was remotely forced from anomalies in the Indian monsoon, whilst our proposal is that anomalous circulation is a direct response to Med-SST anomalies. In contrast, this finding is different from the mechanism found by Rowell (2003) and Jung et al. (2006), who suggested that the Mediterranean influence on WAM system is, via climatological circulation, related to advection of humidity content associated with enhanced evaporation.

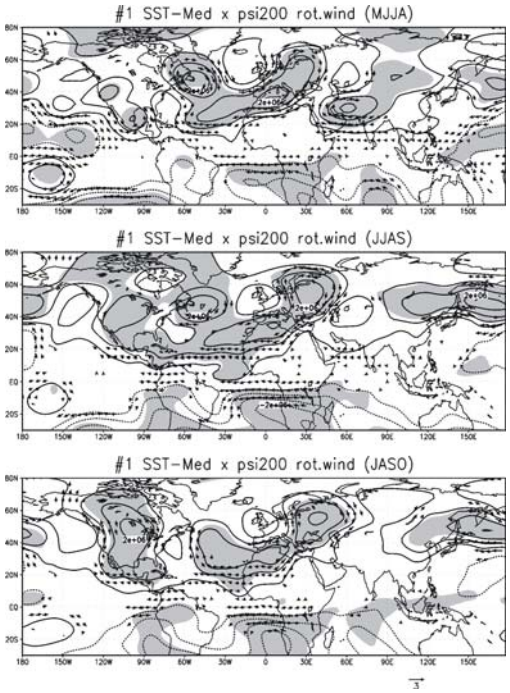


Figure 7. Regression maps of the streamfunction (contours; ci=1x10$^6$ m$^2$/s) and rotational wind (arrows; m/s) onto the EMCA-SST expansion coefficient for MJJA [top], JJAS [middle] and JASO [bottom]; ERA40 dataset for 1979-2001 time-period. Magnitudes correspond to one std of the time series. Vectors are restricted to grid points where at least one wind component exceeds the significance level. Statistically significant areas, according to a *t*-test at the 98% level, are gridded for vectors and shaded for contours.

Another issue which was addressed in García-Serrano et al. (2007) is the answer to the following question: How is the anticyclonic circulation originated and maintained?

There (as in Fig. 7), from a global-scale approach, an almost similar atmospheric anomaly appears over subtropical Atlantic-central Europe during the three selected seasons, involving an extended anticyclone with two closed lobes. In addition, it can be seen that the response has a more global significant signature; indeed, it is apparent that the EMCA-related atmospheric anomalies are essentially confined along the Northern Hemisphere midlatitudes. Also there, the resemblance between 200hPa streamfunction anomaly (Fig. 7) and the simulated wintertime-response shown by Li (2006) made us to suggest that the anticyclonic anomaly is part of a circumglobal teleconnection pattern as a direct response to the Mediterranean warming.
Later, according to the encouraging results by Kodera and Kuroda (2003) and Watanabe (2004), concerning the key role played by the Mediterranean Sea on the hemispheric AO pattern, the explanation became plausible also in observations.

Recently, Jung et al. (2006) have simulated a midlatidude wavelike feature extending from Europe to North America in response to summer Mediterranean SST, but forcing with SST anomalies maximum in the western part of the basin, overlooking the relationship between the global circulation and the WAM system. Finally, Ding and Wang (2005) have evidenced a recurrent circumglobal pattern in summertime, similar to that found by Branstator (2002) for winter, and giving certain robustness to our hypothesis.

Hence, the main task of this study is to investigate the reliability of the large-scale response to Mediterranean SST anomalies in the frame of a hemispheric pattern and based on the EMCA results (for its connection to Sahelian precipitation).

The atmospheric teleconnection patterns that are associated with circumglobal character present low-frequency covariability between very widely separated points, namely the trapping and focusing effects of the time-mean tropospheric jets as they act as waveguide (Hoskins and Ambrizzi 1993, Branstator 2002, Watanabe 2004, Ding and Wang 2005). Theory, observations and model evidences reveal that these effects would not produce zonal mean anomalies but rather zonally oriented chains of perturbations. Next, we analyze the anomalous circulation associated with EMCA-Med in relation to this waveguiding effect.

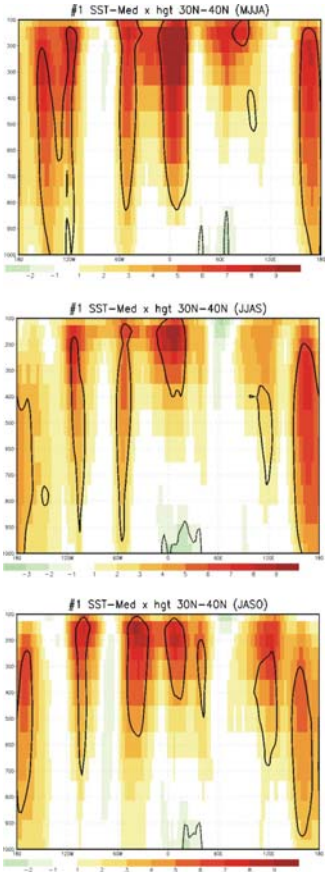


Figure 8. Regression vertical profiles of the EMCA-SST expansion coefficient on the 1000hPa-100hPa anomaloous geopotential height (shaded; m) averaged over 30N-40N; ERA40 dataset for 1979-2001 time-period. Magnitudes correspond to one std dev of the time series. Statistically significant areas, according to a *t*-test at the 98% level, are contoured.

The first step for testing our hypothesis is to localize the local forcing of the atmospheric pattern. Fig. 8 points out the longitude-by-height profile, averaged over the 30N-40N latitudinal window (along the Mediterranean Sea axis), of the anomalous geopotential height regressed onto the EMCA-SST time series. Consistent with the surface warming showed above (Fig. 4; the Med-SST evolution), it is evident the local geopotential negative anomalies over the Mediterranean basin, reflecting the low-level convergence associated with a thermal sea-air forcing. As can be also seen, such a lower-response is accompanied by positive geopotential anomalies (anticyclonic circulation) in the upper-troposphere, involving a local baroclinic structure (maximum in JJAS). It should be note that, except for this local baroclinic anomaly, the atmospheric circulation shows a quasi-barotropic structure worldwide along the Northern Hemisphere midlatitudes.

Additionally, it is important to notice the persistent positive anomaliy (anticyclonic anomaly too) in the North Pacific basin, roughly over 150E-180E, for the subsequent discussion about the connection with the PDO.

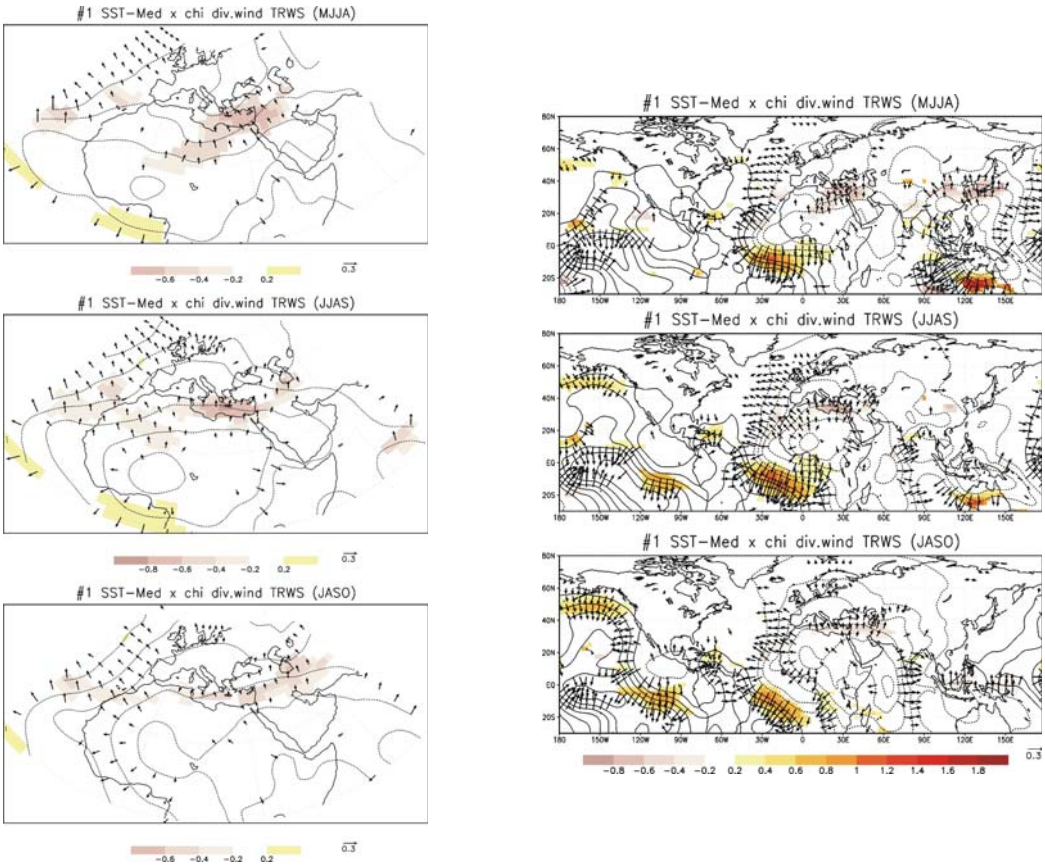


Figure 9. Regression maps of the TRWS (shaded; ci=x$10^{-11}$ $s^{-2}$), velocity potential (contours; ci=1 $10^5$ $m^2$/s) and divergent wind (arrows; m/s) onto the EMCA-SST expansion coefficient; ERA40 dataset for 1979-2001 time-period. Magnitudes correspond to one std dev of the time series. Vectors are restricted to grid points where at least one wind component exceeds the significance level. Only statistically significant areas, according to a *t*-test at the 98% level, are plotted.

Once the local atmospheric column has been evidenced as a response for the Mediterranean forcing, we have to analyze the effective upper-tropospheric forcing, related to the latter, in exciting Rossby waves. Thus, from a preliminar study (not shown here) we have found that larger RWS anomalies correspond to TRWS term (associated with baroclinic anomaly; Fig. 9) rather than ERWS term (associated with

barotropic anomaly). This finding is in agreement with Sardeshmukh and Hoskins (1988), Qin and Robinson (1993) and Renwick and Revell (1999) who pointed to TRWS as major contributor for this sort of thermal-forcing, reflecting the importance of the strong vorticity gradients in the vecinity of the subtropical jets. According to this, this finding follows, on the one hand, the reasoning of the circumglobal response to Med-SST anomaly (Li 2006; with a clear baroclinic strucutre) and, on the other hand, the hemispheric argument as result of Rossby-waves excitation by the anomalous upper-level convergence over the Mediterranean Sea (Watanabe 2004; barotropic structure related to the NAO/AO).

As can be seen, the largest values of TRWS in the Northern Hemisphere (the Summer Hemisphere) are just over the Mediterranean surrounding region, concretely along the southeast flank of the basin. These anomalies, persisting during the three EMCA-lags, are associated with the strong vorticity gradient in the entrance of the NAA jet, reflecting the effective perturbation of the flow.
Thus, to continue with our hypothesis, the possible circumglobal teleconnection (Fig. 8) would be reflecting the result of Rossby wave propagation from a stationary vorticity source produced by upper-tropospheric convergence (anticyclonic anomaly) over the Mediterranean region of thermally-driven convection (Hoskins and Ambrizzi 1993, Li 2006).

In addition, from the global regression of the divergent fields (Fig. 9-right), it is worthy to note both the perturbation in the local ITCZ over the tropical West Africa (for its connection with the WAM-Sahelian rainfall) and the increasing amplitude of the positive TRWS over the North Pacific (from MJJA to JASO) associated with the upper-tropospheric anticyclone commented above (for its connection with the PDO variability; also Fig. 8).

In order to test our waveguiding mechanism for the atmospheric circulation related to the EMCA-Med warming, we have to evidence the trapped anomalies propagation. Fig. 10 shows the geopotential anomalies at 200hPa (Z200) and the westerly mean jet in the three EMCA seasons. It is evident that the Z200 anomalies are mostly confined along a wide-latitudinal band, extending to the entire Northern Hemisphere midlatitudes and reflecting the downward extension into the westerly jet.

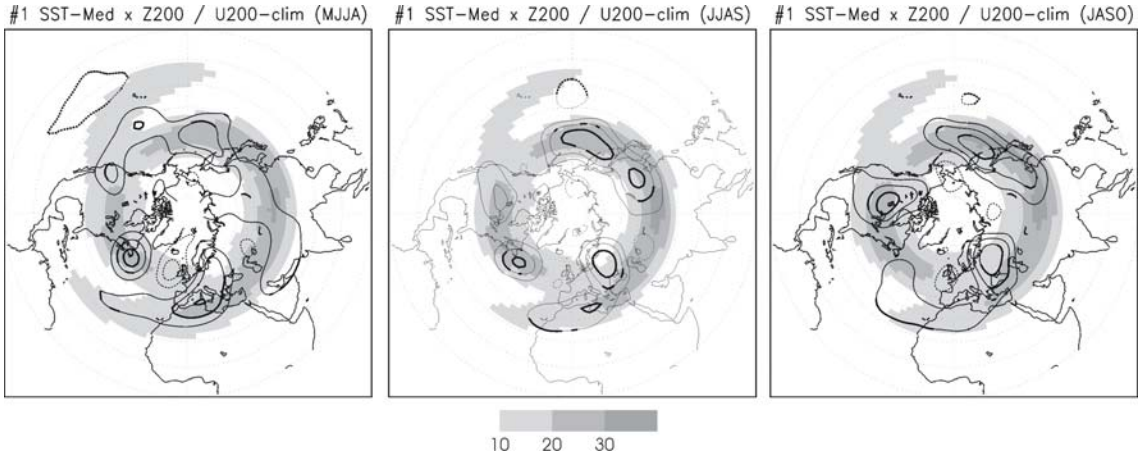


Figure 10. Regression maps of the anomalous geopotential height at 200hPa (contours; ci=5 m) onto the EMCA-SST expansion coefficient overplotted to climatological Northern Hemispehre westerly jet (shaded; ci=10 m/s); ERA40 dataset for 1979-2001 time-period. Regression-magnitudes correspond to one std dev of the time series. Regressed significant areas, according to a *t*-test at the 98% level, are bolded.

Such a zonally oriented wavetrain is reminescent of that one from the winter simulation by Li (2006). Although this mechanism is more active in winter-spring (Branstator 2002), it seems to be at work also in summer-autumn from the EMCA-Med, according to recent results by Ding and Wang (2005) and Jung et al. (2006).

Following the same line of reasoning of Li (2006), teleconnections with strong zonal characteristics are found trapped into the subtropical jet-stream to the North Pacific and North American continent, propagating further across the North Atlantic towards Northern Europe, following the dominant westerly climatology. These remote anomalies are also evident in the regressions at 700hpa (Fig. 11-left) and surface (Fig. 11-right).

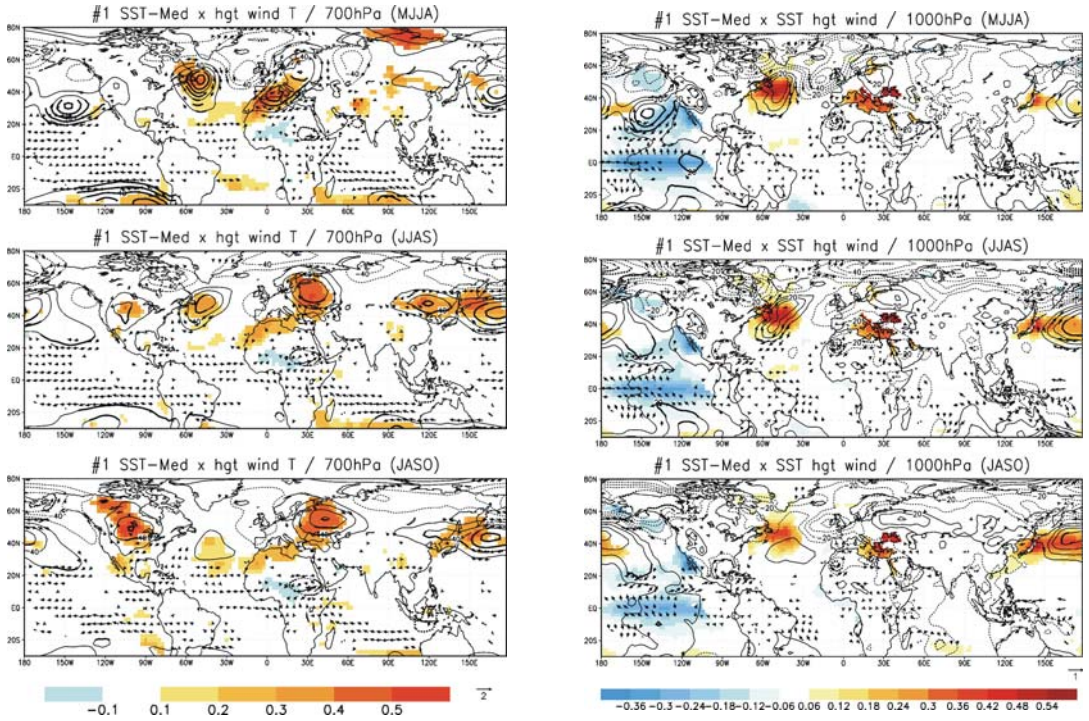


Figure 11. Regression maps of the anomalous geopotential height (contours; m/9.8) and horizontal wind (arrows; m/s) at 700hPa [left] and 1000hPa [right], air temperature at 700hPa (shaded, left; ºC), and SST (shaded, right; ºC) onto the EMCA-SST expansion coefficient. Magnitudes correspond to one std dev of the time series. Vectors are restricted to grid points where at least one wind component exceeds the significance level. Stistically significant areas, according to a *t*-test at the 98% level, are gridded for shading and vectors and bolded for contours.

As can be seen, the upper-tropospheric wavy anomalous circulation becomes diffuse as approaching the surface. Even so, it is evident the Med-impact on both northeastern oceanic basins. It is also important to notice the significant lower-tropospheric warming over Europe (Fig. 11-left) as result of downstream propagation of Rossby-anomalies at the jet exit of the North Atlantic westerly-stream (Ding and Wang 2005).

Likewise, having found that the EMCA signature of jetstream-trapped covariability between widely spaced points in the summer circulation is quite prominent, it seems possible that this mechanism may influence in the low-frequency of the westerly jet itself. To this aim, we have analized both the eddy activity and the wave-mean interaction.

The actual propagation characteristics of the high-frequency transients themselves can be described by the horizontal component of the Eliassen-Palm flux, the E-vector, which gives a description of the interaction between synoptic eddies and the mean flow due to barotropic processes (Hoskins et al. 1983, Trenberth 1986):

$$\vec{E} = \left( \frac{1}{2} \overline{v'v' - u'u'}, \quad -\overline{u'v'} \right)$$

where a prime denotes a deviation from the time mean and overbars a monthly average. These *u'* and *v'* perturbations are calculated by using the 24-h difference filter described in Wallace et al. (1988). The E-vector is approximately parallel to the group velocity (relative to the mean flow) of barotropic Rossby waves and also gives information about the shape and propagation features of eddies. To measure the amplitude of the transient activity we have calculated the perturbation kinetic energy (PKE; also Matthews and Kiladis 1999a-b):

$$PKE = \frac{1}{2} \left( \overline{u'u' + v'v'} \right)$$

Fig. 12 points out the regressions maps of these diagnostics onto the EMCA-SST expansion coefficient. From PKE results, it is clearly evident that the small regressed amplitude indicates the scarce effect on the time-mean tropospheric jet, according to Branstator (2002) in relation to this sort of teleconections. However, the EMCA-Med circumglobal propagation-pattern is associated with E-vectors showing an east-west orientation, depicting a elongated axis of Rossby perturbations and corfirming the zonally oriented wavetrain. Such a feature, the absence of an apparent meridional component, also reflects that there is not a net influence on the main westerly jetstream.

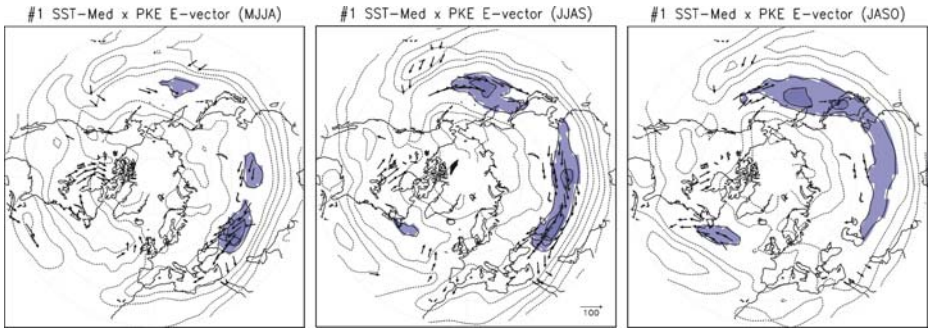


Figure 12. Regression maps of the anomalous PKE (contours; ci= 20 $m^2/s^2$) and E-vector (arrows; $m^2/s^2$) at 200hPa onto the EMCA-SST expansion coefficient; ERA40 dataset for 1979-2001 time-period. Magnitudes correspond to one std dev of the time series. Vectors are restricted to grid points where at least one wind component exceeds the significance level. Stistically significant areas, according to a *t*-test at the 98% level, are shaded for contours and gridded for vectors.

According to evidences shown above, there is also a marked influence on the western North Pacific basin, increasing in amplitude in the course of time (from MJJA to JASO). To establish a statistical link between the EMCA-Med circumglobal pattern and the PDO variability, we have calculated the correlation of the EMCA-SST expansion coefficient with the seasonal PDO index* (Fig. 13).

* Obtained from http://www.jisao.washington.edu/pdo/

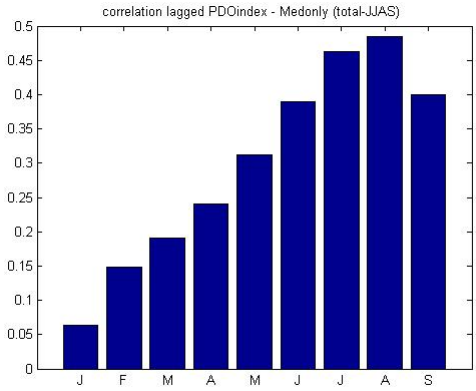


Figure 13. Correlation coefficient between the EMCA-SST time-series and the seasonal PDO index from JFMA to SOND (indicated by the first month of the 4-months sequence).

As it is evident, and following the same line of reasoning from above results (Figs. 7-to-12), the relationship between the Mediterranean SST time-evolution and the seasonal PDO index strenghthens as the circumglobal teleconnection is likely developed (clearly seen in JJAS-JASO). Even so, as reveled from Fig. 13, the maximum correlation with the North Pacific phenomenon occurs during ASON. However, such a finding is in agreement with the idea of an extratropical atmospheric forcing (remotely triggered from the Mediterraean region) of a midlatitude oceanic anomaly. In short, the barotropic teleconnection centre over the North Pacific, associated with an anomalous anticyclone, results in either an enhanced subsidence in the northeastern basin or a surface anticyclonic circulation, producing less evaporation and warm northward advection thereby increasing both the positive SST anomalies and the connection with PDO variability. This atmosphere-ocean direct mechanism has been determined by several studies (e.g. Bladé 1997, Frankignoul et al. 1998), establishing the time-lag of the forcing in approximately one month, in complete agreement with EMCA-Med results.

This relevant finding opens the possibility of including the Mediterranean anomalous state in the potential predictability on the PDO variability, and, consequently, also on the ENSO variability (e.g., Gershunov and Barnett 1998, Barnett et al. 1999).

## Remote link between the Mediterranean mode and the WAM variability

Now, we tackle the remote impact of the EMCA-Med on the WAM system. As it is well known, the Mediterranean is a boundary region that feels both the dynamics of the tropical circulation cells and the mid-latitude stationary waves. Thus, the seasonal cycle is consequently very important, since it regulates the transition from the winter regime, dominated by mid-latitude circulation, to the summer regime, characterized by the tropical dynamics (Raicich et al. 2003). Contemporary to the latter, the WAM monsoon develops its peak phase (Sultan and Janicot 2000, Janicot and Sultan 2001). In accordance with a number of works, due to its particular geographical position under the descending motion of the local Hadley circulation, the Mediterranean Sea is a potential player on the African monsoon season (Fontaine et al. 2003, Raicich et al. 2003, Rowell 2003, Jung et al. 2006, Fontaine et al. 2008).

Fig. 14-left shows the EMCA-Med precipitation related to the WAM-Sahelian rainfall. It is important to bear in mind that the EMCA-precipitaion expansion coefficient (JJAS) is 0.96 correlated with the first WAM-EOF (JJAS), the Sahelian mode (Polo et al. 2008).

On the one hand, and as it is noticeable, the WAM precipitation anomalies associated with EMCA-Med are not restricted to the peak season of the monsoonal rainfall (JJAS); pointing out a clear reminiscent pattern in both MJJA (one negative lag) and JASO (one positive lag), and giving certain robustness to the connection found. Whereas the JJAS positive anomalies extend to the entire Sudan-Sahel area, the lagged ones are practically confined to 20E-surrounding region.
On the other hand, and according to the seasonal correlation coefficients shown in Fig. 6, the EMCA-Med results in this scenario suggest a certain predictability in the influence on WAM system, indicating a possible trigger role of the Mediterranean.
Jointly, the spatial patterns and the temporal relationship (MJJA-to-JASO), could reveal the likely weight in the teleconnection between the Mediterranean-related SST anomaly (maximum over the eastern basin) and the WAM precipitation (Sahel region); pointing the impact to 10E-30E longitudinal band.

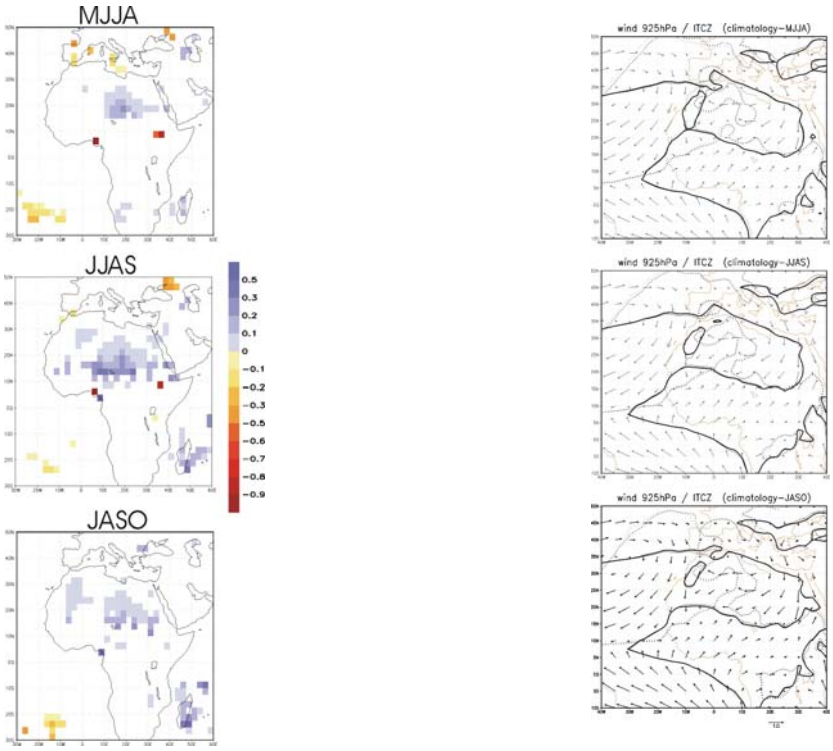


Figure 14. [left] Regression maps of the CMAP precipitation anomalies (mm/day) onto the EMCA-SST expansion coefficient. [right] ERA40 climatology of the 925hPa horizontal wind (arrows); contouring the zonal-zero value (solid) and the meridional-zero value (dashed), as proxy of the ITCZ. Regressed-magnitudes correspond to one std dev of the time series. Only stistically significant areas, according to a *t*-test at the 98% level, are plotted for rainfall (left pannel).

In the preliminary study (García-Serrano et al. 2007), the authors proposed a mechanism for explaining the Med-WAM relation which had involved the reinforcement of the TEJ (at upper-tropospheric levels). However, such tropical circulation-anomaly is absent in this refined analysis. There, the southward extension of the large-scale anticyclone as response to Med-SST warming (Fig. 7) was suggested as connector-agent with the Sahelian rainfall. On the contrary, the regressed profile of the anomalous zonal wind (averaged between 10E-30E; Fig. 15-right) rules out this hypothesis, because the TEJ is mostly located just over the ITCZ-related deep convection (Grist and Nicholson 2001, Nicholson and Grist 2001). In the same way, there is no evidence for considering the African easterly jet (AEJ; at mid-tropospheric levels) anomaly as precursor of WAM precipitation, since the anomalous easterly wind

in that location is maximum during JASO when the Sahelian rainfall vanishes; reflecting that the AEJ anomalous state is a consequence of the ITCZ activity rather than cause (Cook 1999, Hsieh and Cook 2005, Berry and Thorncroft 2005, Hall et al. 2006, Mekonnen et al. 2006).

Above results made us focus the analysis on others elements governing the WAM system, like the ITCZ-associated local Hadley cell and the westerly monsoonal flow. Fig. 14-right and Fig. 15-left show the climatological circulation in the WAM region during the seasonal monsoon regime (from MJJA to JASO); pointing out, respectively, the horizontal and meridional-vertical circulation climatologies. As established, the meridional-vertical circulation cell (local Hadley cell) shows a dramatic shift between winter and summer, indicating a displacement of the convective area from 5S-5N to the 10N-15N (e.g. Raicich et al. 2003). The low-level southern branch of this Hadley cell is composed of northly wind regimes longitudinally-known as Harmattan (mid-Med) and Etesian (east-Med) (e.g. Jung et al. 2006).

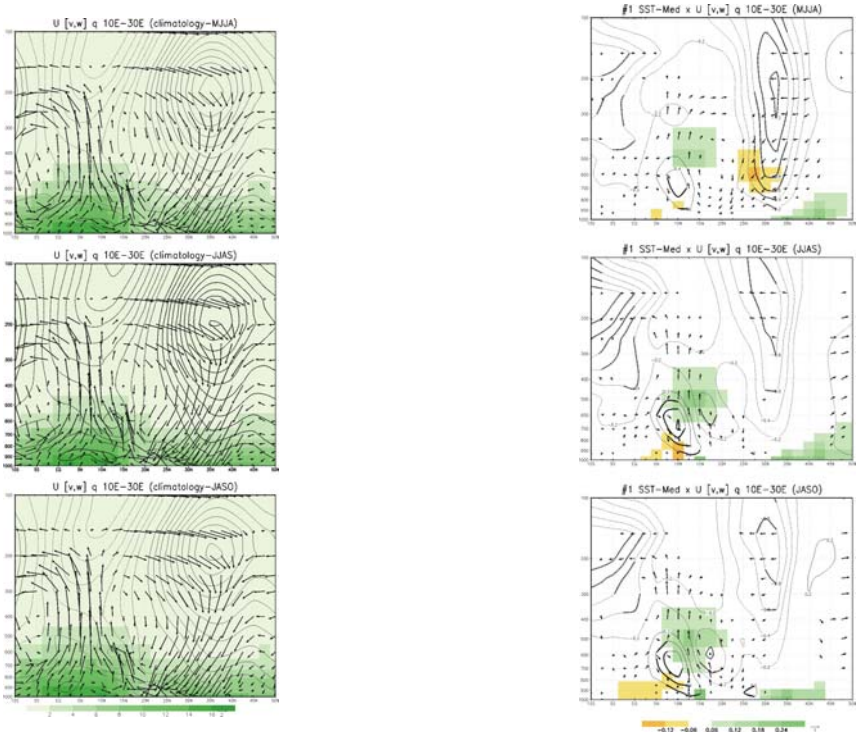


Figure 15. [left] Vertical-profiles climatology of the ERA40 zonal wind (U; contours, m/s), meridional (m/s) and pressure-vertical (x (-100) hPa/s) winds (v,w; arrows) and specific humidity (q; shaded, 1000 x g/g) averaged over 10E-30E. [right] Regression profile-maps of ERA40 U, v, w and q 10E-30E averaged anomalies onto the EMCA-SST expansion coefficient. Regressed-magnitudes correspond to one std dev of the time series. Regressed-vectors are restricted to grid points where at least one wind component exceeds the significance level. Regressed-statistically significant areas, according to a *t*-test at the 98% level, are gridded for shading and vectors and bolded for contours (right pannel).

Another important climatological-dynamic factor influencing the interannual variability of WAM-Sahelian rainfall is the westerly monsoon flow, or monsoonal flow, in charge of advecting the tropical Atlantic humidity (Fig. 14-right). In fact, these off-equatorial westerlies significantly modulate the Sahel-interannual variability (Grist and Nicholson 2001). Even more, there is evidence indicating that the degree of development of westerlies is the major contrast between wet and dry years (Nicholson and Grist 2001).

As commented above, EMCA-Med analysis is associated with a clear and significant deceleration of the subtropical westerly jet, instead of a perturbation in the TEJ essentially not found (Fig. 15-right). Such a feature, as evidenced from the large-scale approach, is related to the upper-tropospheric anomalous anticyclone as thermally-driven response to Mediterranean EMCA-SST (Figs. 7, 8, 10).
Additionally, in order to characterize the Sahelian rainfall variability, we can observe contemporary both, an above-normal convergence of moisture occuring into the ITCZ (centred at 500hPa/10N-15N) and a strenghthening and deepening, rather than northward displacement, of the westerly monsoon flow (5N-15N, 900hPa-500hPa). Contrary to the latter, the former is accompanied by an apparent northward migration of the deep-vertical motions [and humidity content]; vertical-axis displaced from 5-7N [7N] to 7-10N [13N] (Fig. 15).

As proposed by Rowell (2003), warmer than average SSTs in the eastern Mediterranean lead to enhanced local evaporation, and hence to enhanced lower-tropospheric humidity there (also in Fig. 15-right). However, from EMCA-Med results there is not evidence of its advection across the arid eastern Sahara, which would feed enhanced moisture convergence over the Sahel and hence enhanced rainfall. Note that, although Rowell's model simulation was performed with a similar SST forcing to EMCA-SST anomaly, his resulting precipitation pattern had the loading scores to the west of 0E with maximum anomaly off African coast (his Fig. 8), completely opposite to findings shown here (Fig. 14-left).

The main features in the EMCA Med-WAM teleconnection, added to anomalous subtropical easterly flow, are the intensification of the ITCZ and the increase of monsoonal westerlies (Fig. 15-right). In the Sahelian rainfall-variability scenario, the latter is closely associated with the former, causing the enhancement of lower-tropospheric moisture advection inland the African continent (Fig. 14-right) and resulting in above-normal rainfall over the Sahel (Fig. 15-left) (e.g. Jung et al. 2006)
.
According to this, Grist et al. (2002) found that the horizontal shear, rather than the vertical one, is more important in causing the differences between wet and dry years. On the contrary, these results differ from those pointing to the relationship between TEJ and AEJ governs both the extent of the rainbelt and its intensity (Nicholson et al. 2007, Nicholson et al. 2008, Nicholson 2008). Even so, it is should be mentioned that the weakly increased easterly wind in the AEJ during JJAS (Fig. 15-right, middle) could further favour the horizontal shear, thereby likely increasing the instability and allowing African easterly waves (AEWs) to develop downstream. However, we suggest that further increase of Sahelian rainfall based on AEWs activity comes from cumulus convection within the ITCZ (prominent in MJJA-JJAS) and not by shear associated with the AEJ, following the argument by Hsieh and Cook (2005), Berry and Thorncroft (2005) and Mekonnen et al. (2006). Results from GCM simulations (Cook 1999), identifying the cause of the AEJ as the soil moisture distribution, are in agreement with the consequence-role of the AEJ to enhanced Sahelian precipitation.

Consequently, and according to EMCA-Med results, Giannini et al. (2003) pointed out that the SST variability is crucial in determining the sign of rainfall anomalies in the Sahel, whereas coherent land-surface interaction acts to amplify them. Summarizing, the Mediterranean summer SST anomaly has been found strongly correlated with Sahel rainfall anomalies, involving the reinforcement of both ITCZ-deep motion and ocean-land westerly transport of humidity thereby, in short, strenghthening the main WAM circulation regime which leads to enhanced seasonal rainfall.

Finally, one would wonders what is exactly the responsible mechanims in the WAM-Sahel precipitation linked to Mediterranean SST anomaly. To answer this question, and in order to characterize the EMCA-Med large-scale features in the Sahelian rainfall variability, it is important to look at the anomalous state of the local Hadley cell; as noted down by Raicich et al. (2003), who speculated the physical mechanism may involve variations in the WAM-Sahelian ITCZ. In fact, integral with this tropical main aspect is the tropical-extratropical overturning meridional cell, namely the closed meridional-Hadley circulation.

Thus, Fig. 15-right clearly indicates an important contribution to the ITCZ low-level convergence (15N-25N) from the downward-northly Hadley circulation (25N-30N). Indeed, this descending air seems to be mainly of mid-latitude origin, sinking over the subtropical latitudes related to the anomalous upper-tropospheric easterly jet (200hPa, 30N-35N). To explain this circulation condition, we have referred the model-study of Rodwell and Hoskins (1996). Following this work, we suggest that the anomalous upper-tropospheric anticyclon-associated subtropical easterly flow interacts with the climatological mid-latitudes westerlies causing the air to descend. In such a way, this adiabatic descent, localized over the eastern Sahara and suthern flank of the Mediterranean basin, would be the piece of the puzzle connecting the thermally forced atmospheric response to Med-SST warming (in turn, part of a circumglobal pattern) to above-average Sahelian precipitation anomalies via large-scale circulation of the WAM system (ITCZ-Hadley perturbations).

## *Model representation*

To test the origin of the observational EMCA mode described above for the Mediterranean in relation to the atmospheric response and WAM, different model experiment are needed. On the one hand, to test if the relation comes naturally from the coupled ocean-atmosphere system, we have repeated the analysis with the ocean-atmosphere coupled models currently used at Met Office, applying the same EMCA methodology to the outputs from two different realizations. These are 60-years simulation with the same pre-industrial conditions of two different versions of the HadGEM model, namely the HadGEM1 and HadGEM2. Finally, to test if the relation is SST forced, AGCM experiment with prescribed SSTs are also analysed.

### **Results from HadGEM1**

In HadGEM1, the only statistically significant co-variability mode corresponds to WAM-rainfall anomalies associated with the Guinean Gulf (GG) mode (Fig 16). Such a mode is the leading mode of the EMCA analysis (EMCA1), explains the 51% of the scf between the predictor (FMAM-SOND Med SST) and the predictand (JJAS WAM-rainfall), and has a modest correlation of 0.47 between expansion coefficients. The EMCA1 Med SST associated pattern shows an evolution of the SST anomalies from the western basin in spring (FMAM-AMJJ) to the eastern part in autumn (JASO-SOND). The regression map of the global SST onto the EMCA1-SST expansion coefficient (Fig. 17) has maximum loadings over the equatorial Atlantic (negative SST anomalies); indicating, as expected, the association between GG precipitation and the tropical SST pattern, namely the Atlantic Niño (Janicot et al. 1998, Okumura and Xie 2004, Polo et al. 2008). This result implies that the EMCA1-Med SST pattern would be representing a footprint of the well known coupled phenomenon Atlantic Niño-GG rainfall. Thereby, such a tropical-extratropical relation is linked to an atmospheric teleconnection.

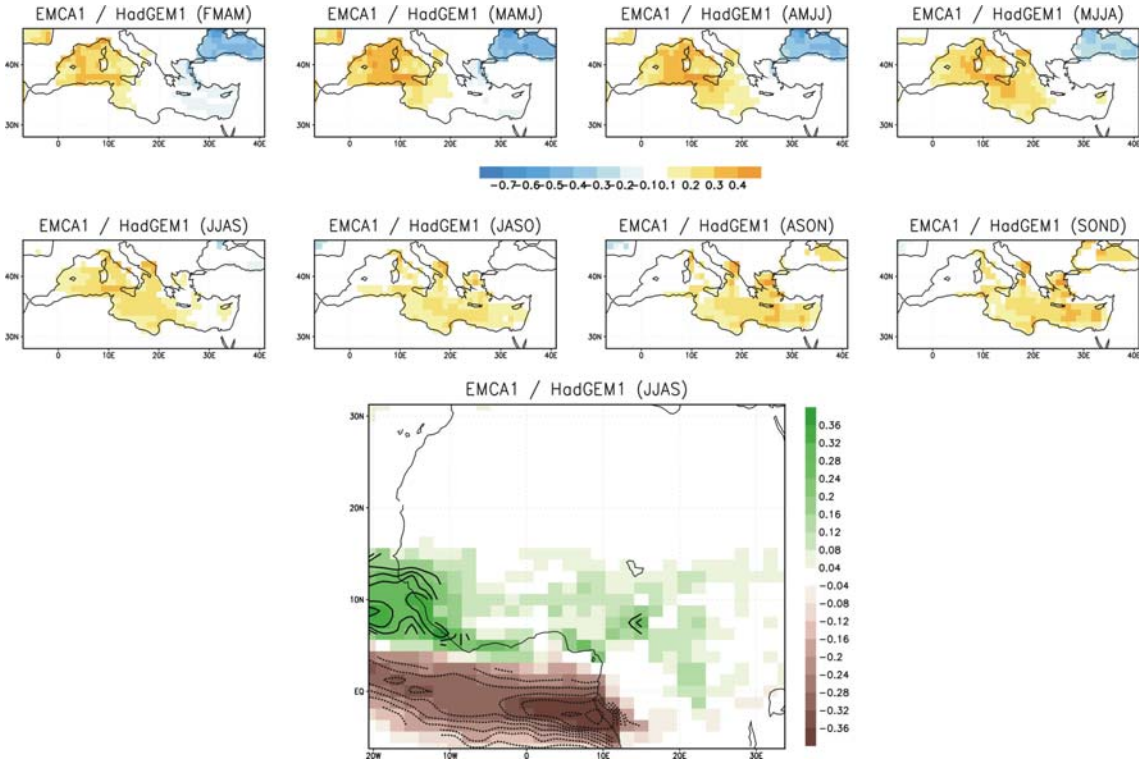


Figure 16. Leading co-variability EMCA mode (EMCA1) between the Mediterranean time-varying SST (FMAM-to-SOND) and JJAS WAM-precipitation applied to 60yrs coupled-run with pre-industrial conditions from HadGEM1. (top-panel) Homogeneous regression maps of Mediterranean SST anomalies (ºC) and (bottom) heterogeneous regression map of the WAM rainfall (std anomalies) onto the EMCA1-SST expansion coefficient. Statistically significant areas, according to a *t*-test at the 98% level, are gridded for SST and contoured for precipitation.

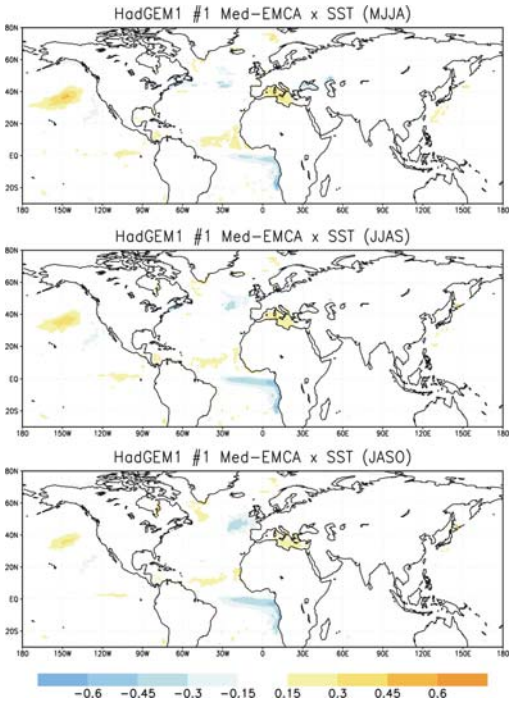


Figure 17. Regression maps of the global SST anomalies (ºC) onto the EMCA1-SST expansion coefficient obtained from 60yrs coupled run with HadGEM1. Magnitudes correspond to one std dev of the time series. Only statistically significant areas, according to a *t*-test at the 98% level, are plotted.

Analyses from lower (1000hPa) and upper (200hPa) tropospheric-levels (Fig. 18) indicate that the Atlantic Niño-Mediterranean relationship could be explained in terms of a quasi-barotropic Rossby wavetrain emanated from the Caribbean region extending along the North Atlantic. Thus, on the one hand, the Atlantic Niño EMCA1-based SST anomalies are associated with above-normal surface pressure anomalies (Z1000) over the eastern equatorial Atlantic and, jointly, negative surface pressure anomalies over Central America; indicating the reinforcement of the seasonal Walker local-cell (Wang 2002, García-Serrano et al. 2008). These perturbations would force an anomalous surface convergent-inflow and an upper-tropospheric divergent-outflow over the Caribbean Sea. Then, on the other hand, the Atlantic Niño EMCA1-based SST anomalies are associated both with positive geopotential anomalies at 200hPa (Z200) in the western tropical Atlantic, reflecting the anomalous vorticity source, and an downstream wavetrain crossing the entire North Atlantic basin towards Europe.

The zonally-oriented SST dipole present at North Atlantic mid-latitudes (Fig. 17), positive (negative) in the western (eastern) part of the basin, may be associated with that Rossby-wave pattern.

Even so, the statistical significance of the teleconnection-centres of action is quite limited (excluding JASO; Fig. 18), hence this proposed mechanism requires further investigation. In fact, another exchange-visit funded by ESF-MedCLIVAR has been recently proposed, from our group at UCM, for continuing this research line.

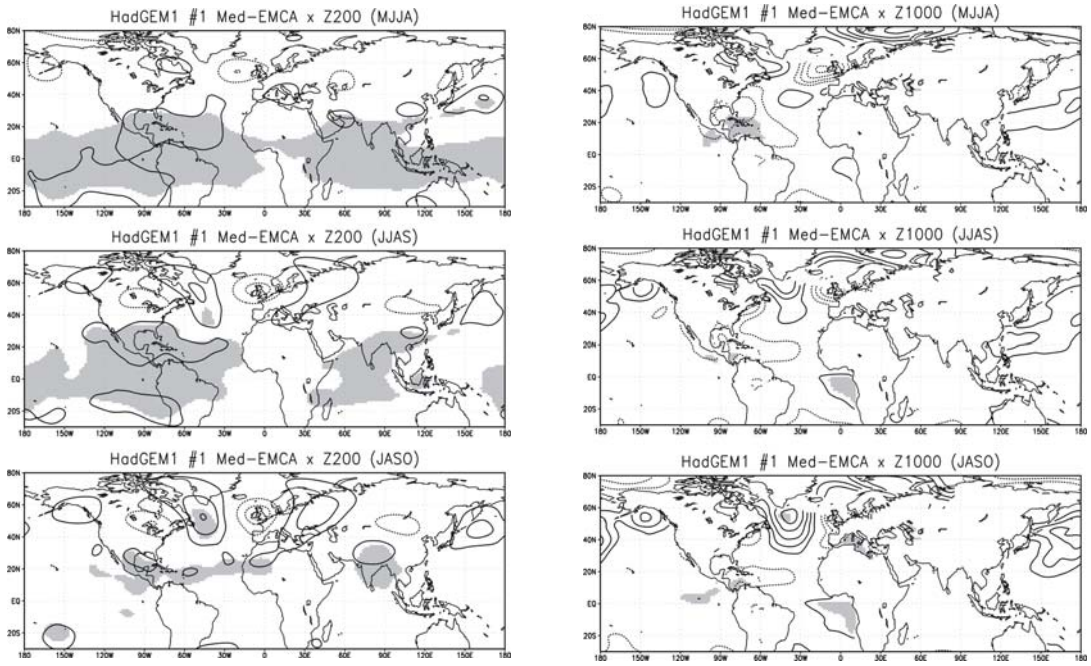


Figure 18. Regression maps of the geopotential height at 200hpa (left; contours, ci= 5hPa) and 1000hPa (right; contours, ci= 1hPa) onto the EMCA1-SST expansion coefficient obtained from 60yrs coupled run with HadGEM1. Magnitudes correspond to one std of the time series. Statistically significant areas, according to a *t*-test at the 98% level, are shaded.

**Results from HadGEM2**

Regarding the results from HadGEM2; the above Atlantic Niño-GG rainfall coupled mode and its relation to the Mediterranean time-varying SST pattern, derived from EMCA-HadGEM1, corresponds to the second covariability-mode (EMCA2) after applying EMCA to the 60yrs coupled run of HadGEM2 (Fig. 19). Here, the explained scf between fields is 23%, whereas the correlation coefficient of the expansion coefficients is 0.38. Overall, these covariability measures related to GG anomalous precipitation are rather low in HadGEM2 than HadGEM1, implicating that the remote relationship is more weakly represented. However, the fact that both HadGEMs coupled-models show the Atlantic Niño-GG rainfall connection with Mediterranean summer SST anomaly implies that this relationship is a robust feature.

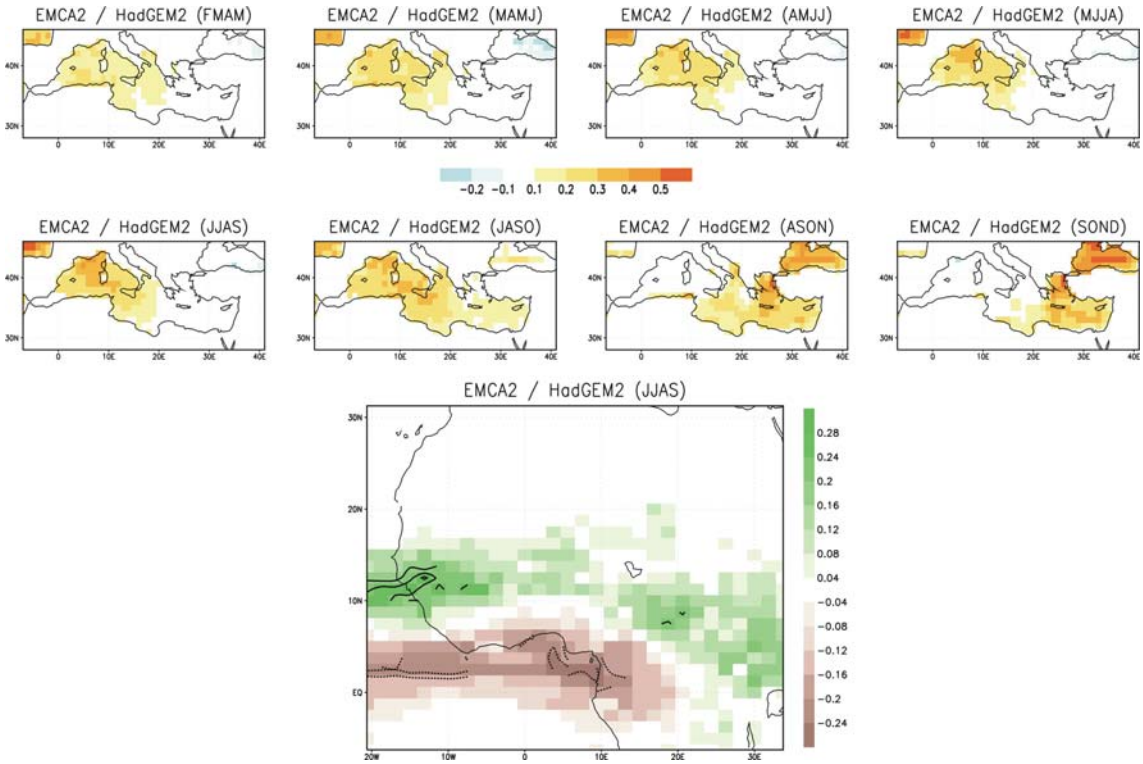


Figure 19. As Fig. 16 but for second EMCA-mode derived from the 60yrs pre-industrial run with HadGEM2.

The leading mode of the Med-EMCA applied to HadGEM2 coupled run (EMCA1; Fig. 20) shows positive precipitation anomalies inland of the GG coastline, roughly over 5W-0E and below 10N. As can be seen, this EMCA1-WAM rainfall pattern, which has a statistical significance quite limited, is so different to the observed Sahelian precipitation anomaly (Figs. 4, 14-left) that it is useless to make comparisons: CMAP-Sahelian rainfall yields positive anomalies east to 0E and between 15N-20N, whilst HadGEM2-EMCA1 depicts above-normal precipitation west to 0E and further into sub-Saharan Africa.

On the contrary, the time-evolving SST pattern in the Mediterranean Sea associated with HadGEM2-EMCA1 points out a common feature regarding Med-EMCA in the observations (Fig. 4), showing the maximum amplitude over the eastern part of the basin. Indeed, according to both observed Med-EMCA (as Polo et al. 2008, her Fig. 9a) and the works by Xoplaki et al. (2003a, her Fig. 6h; 2003b, her Fig. 5c); the HadGEM2-related SST pattern seems to be conditioned by the anomaly in the Black Sea (loading scores), although it also spreads on the Greece-Cyprus surrounding area (Fig. 20).

The above mentioned discrepancy in the Mediterranean-Sahel connection, with similar SST patterns and the different precipitation anomalies, for HadGEM2-EMCA1 and the observed Med-EMCA is an intriguing result. Global regressions using the HadGEM2-EMCA1 SST expansion coefficient give some clues (Fig. 21). The global-SST regression maps (Fig. 21-left) reproduce the observed Med-SST damping during late-summer together with the increasing amplitude of the North Pacific positive SST anomaly (Fig. 11-right). Also it is apparent the increasing negative anomaly in the equatorial Pacific. This finding points again at PDO variability as a phenomenon teleconnected with the Mediterranean SST anomalies; implying very relevant results for the global climate system. The Pacific SST pattern linked to Med-SST differs from the canonical ENSO signal, depicting the maximum equatorial anomalies in the central part of the basin.

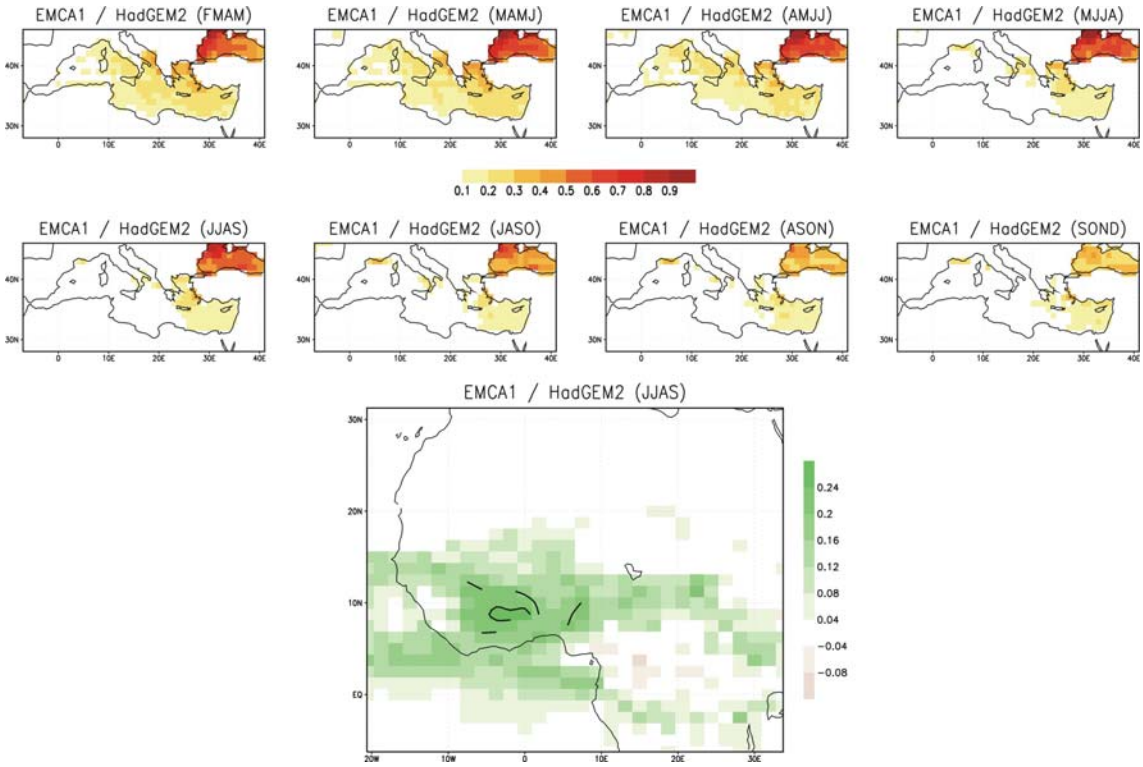


Figure 20. As Fig. 16 but for leading EMCA-mode derived from the 60yrs pre-industrial run with HadGEM2.

The global-Z200 regression clearly shows an anomalous anticyclonic circulation over the maximum SST forcing (Fig. 21-right). The corresponding surface anomalies also show negative pressure anomalies in the Black Sea surrounding region (only statistically significant in MJJA, not shown); indicating, as in the observations, a direct baroclinic response to Med-SST. Likewise, the proposed waveguided atmospheric circulation is present in HadGEM2-EMCA1; resulting in a downstream propagation across the Eurasian continent, trapped into the NAA westerly-jet, that leads to an anticyclonic anomaly over western North Pacific (150E-180) forcing strong subsidence there (MJJA-to-JASO).

Regarding the Med-WAM relationship in HadGEM2-EMCA1, this GG rainfall pattern (Fig. 20) does not seem to be associated with the large-scale atmospheric response to Med-SST anomaly, because the midlatitudes anticyclonic anomaly (at 45N-50N) does not perturb the westerly flow over northern Africa-Mediterranean upper-tropospheric

levels (at 25N-35N; not shown). In fact, the HadGEM2-EMCA1 GG anomalous precipitation seems to be more related to the local ITCZ (local vertical motions, at 10N; Sultan and Janicot 2000) than alterations in the local Hadley cell (no evidence of enhanced returning-subsidence has been found; not shown).

Looking at global-SST regression (Fig. 21-left); besides the possible feedback from subtropical North Atlantic (e.g. Rowell 2003, Polo et al. 2008) or the local increased evaporation from weak positive SST anomalies in the equatorial Atlantic, the evolving negative anomaly in the equatorial Pacific could impact on the HadGEM2-EMCA1 WAM rainfall. Following this argument, previous works have evidenced a negative correlation between WAM-rainfall and ENSO-like equatorial SST, resulting in positive precipitation anomalies in conjunction with negative SST anomalies (La Niña conditions; e.g. Janicot et al. 1998). On this respect, Janicot et al. (1998) suggested that the Pacific-WAM teleconnection could be monitored by a Walker-type zonal circulation over the tropical Atlantic. However, there is no evidence for such kind of surface-pressure dipole between the tropical Pacific and Atlantic basins; only positive Z1000 anomalies have been found over the central-eastern Pacific (not shown). Alternately, Rowell (2001) proposed that such a teleconnection could result from anomalous stationary equatorial Kelvin-waves propagating from the Pacific, either through a direct influence of the vertical motions on convection, or through a perturbation in the North Africa anticyclone leading to a moisture advection anomaly. Regardless of these interpretations, the concomitance of negative tropical Pacific SST anomalies with positive ones in the equatorial Atlantic could enhances the inter-basin zonal gradient between the eastern Pacific and tropical Atlantic and, then, would lead to above-normal precipitation anomalies over West Africa.
This Pacific-WAM climate link, including the potential role of the Mediterranean Sea via PDO variability, represents a very daring challenge which must be tackle with designed OAGCM-sensitivity experiments.

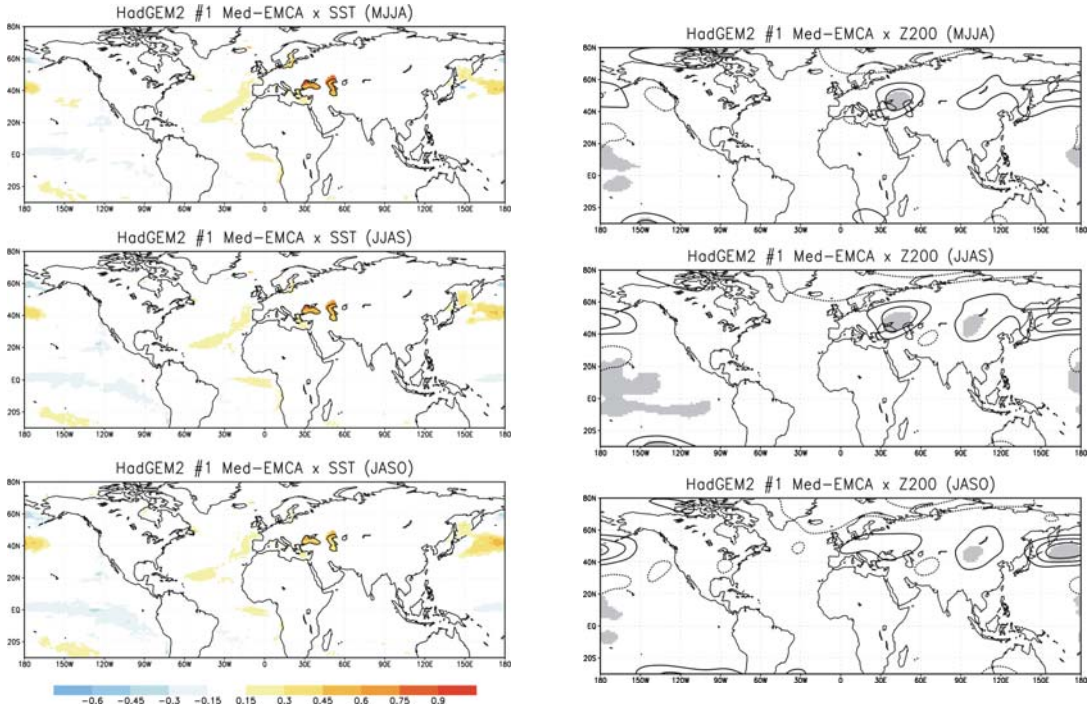


Figure 21. Regression maps of the global SST (left; shaded, ºC) and geopotential height at 200hpa (right; contours, ci= 5hPa) onto the EMCA1-SST expansion coefficient obtained from 60yrs coupled run with HadGEM2. Magnitudes correspond to one std dev of the time series. Statistically significant areas, according to a *t*-test at the 98% level, are gridded for shading and shaded for contours.

This far, there have been no evidence for reproducing in HadGEM's family the eastern Mediterranean SST-Sahelian rainfall connection derived from observations. Not so, HadGEM2 seems to be capturing some indication of large-scale atmospheric response to summer Mediterranean SST anomaly, which is really an encouraging finding.
Regarding the former, it is worthy of noting that Joly et al. (2007) emphasized the OAGCMs' difficulty in simulating the African monsoon rainy-season, particularly the Sahelian rainfall. Thus, from this scenario, the absence of the Med-Sahel connection in both 60yrs pre-industrial coupled runs (HadGEM1 and HadGEM2) make us think that the observed WAM trends could be partly a response to the anthropogenic forcing, according to Held et al. (2005), Biasutti and Giannini (2006), Joly et al. (2007); and in contrast to Giannini et al. (2003), Hoerling et al. (2006). Even so, it is important to bear in mind that the response of the WAM precipitation is still highly model-dependent (Joly et al. 2007, among others).

All above suggests the need for a more detailed validation of the WAM variability, including the overlooked dynamical-link between Mediterranean and the WAM-Sahel rainfall, as well as the large-scale atmospheric response to Med-SST anomalies.
In this respect, validating SST-rainfall teleconnections is particularly attractive for at least two reasons. On the one hand, such teleconnections clearly contribute to the observed climate variability at interannual and multi-decadal time scales and their evolution might therefore influence the twenty-first century climate projections. On the other hand, such teleconnections are mainly controlled by the large-scale atmospheric dynamics and therefore represent much more than a validation of SST and rainfall variability.

## Results from an Atmospheric General Circulation model

Next we have applied the same EMCA methodology to an AGCM large-simulation using the UCLA model and prescribing 1979-2005 observed SST. A detailed description of this simulation is given in Mohíno et al. (2008). Note that this AGCM simulation extends the Med-EMCA observational time-period for four years, from 2001 to 2005. Fig. 22 shows the leading covariability mode of the Med-EMCA derived from the UCLA prescribed-run (AGCM-EMCA), which takes into account almost the 45% of the scf and presents a correlation of 0.70 between SST time-varying predictor (FMAM-to-SOND) and WAM-rainfall predictand (JJAS). As in observations, such a performance has been obtained after detrending SST and precipitation dataset, and additionally standardizing the precipitation anomalies.

As can be seen, AGCM-EMCA1 fairly captures the evolution of the Mediterranean SST pattern from observations (Fig. 4), but slightly points out a major weight in the central part of the basin. Regarding the associated WAM anomalies; the AGCM-EMCA yields the Mediterranean-related Sahelian rainfall quite accurately, although with statistical limitations. Excluding the detrending in the model-EMCA computation (Fig. 22, bottom-right), the statistical significance is largely improved (scf=69%; ruv=0.79). However, the climate implications of the difference in forcing the AGCM model with detrended-SST and detrending the outputs after forcing with un-detrended SST is out of the scope of this work. Such a issue requires further investigation (and an additional large-simulation with detrended SST forcing).

Fig. 23 illustrates the structure of the general atmospheric circulation which enables to explain the large-scale Med-teleconnection (Fig. 23-left) and the mechanism between the Mediterranean SST and the West African monsoon (Fig. 23-right).

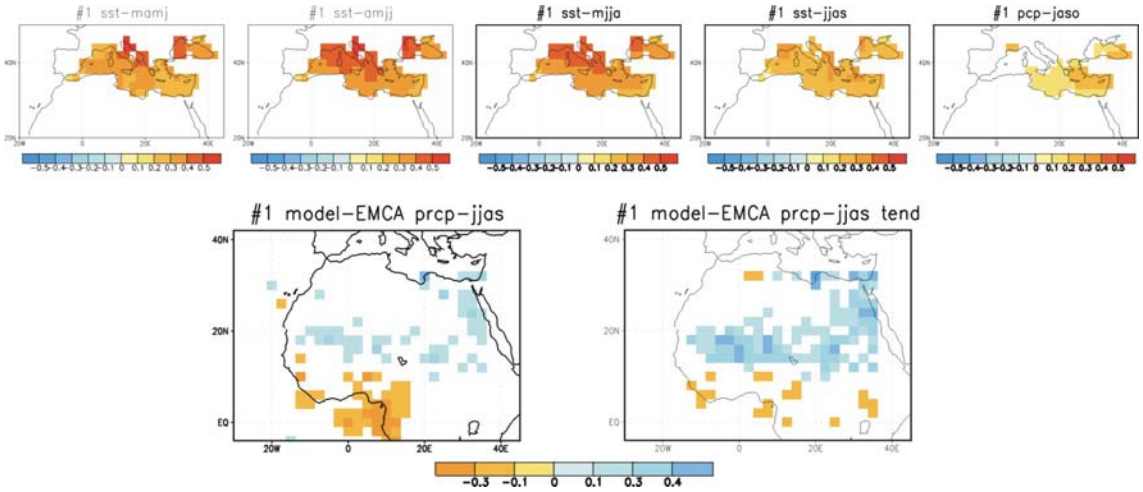


Figure 22. Leading co-variability mode (AGCM-EMCA) of the Mediterranean time-varying SST (FMAM-to-SOND) and JJAS WAM-precipitation EMCA analysis applied to 1979-2005 observed SST UCLA-AGCM simulation. (top) Homogeneous regression maps of Mediterranean SST anomalies (ºC) from MAMJ-to-JASO EMCA-sequences, and (bottom) heterogeneous regression maps of detrended (left) and un-detrended (right) WAM rainfall (std anomalies) onto the corresponding AGCM-EMCA SST expansion coefficient. Only statistically significant areas, according to a *t*-test at the 98% level, are plotted.

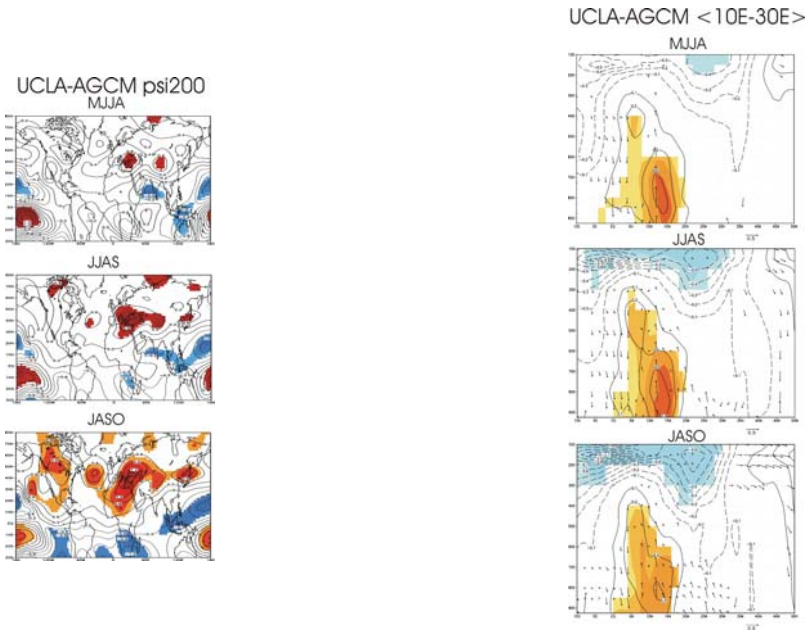


Figure 23. [left] Regression maps of the streamfunction at 200hPa (contours, ci=0.1 $10^6$ $m^2/s$); and [right] regressed-vertical profiles of zonal wind (contours, ci=0.1 m/s), meridional (m/s) and omega (x –100, hPa/s) (arrows) onto the AGCM-EMCA SST expansion coefficient. Magnitudes correspond to one std dev of the time series. Statistically significant areas, according to a *t*-test at the 98% level, are shaded for contours and gridded for vectors.

The former confirms both, the local baroclinic structure in response to summer Med-SST anomaly, low-level convergence (not shown) and upper-tropospheric anomalous anticyclone; and the downstream propagation into the westerly jet as part of the circumglobal teleconnection, with action-centres in Eurasia and over western North Pacific (Japanese islands). Note, as in observations (Fig. 7), the evolution of the local positive streamfunction anomalies over the Mediterranean basin and the time-increasing amplitude of the anomalous anticyclone over Japan (MJJA-to-JASO).

The latter shows the enhanced Sahelian convection and the strong-deep degree of development of the (westerly) monsoonal flow (5N-15N; Fig. 23-right). Also it is evident the influence of the anomalous midlatitudes easterly-flow (related to above anticyclonic response) on the regional WAM climate; entailing the intensification of the overturning anomalous Hadley cell (above all at 25N-35N). This fact represents a first confirmation of the large-scale impact of the Mediterranean Sea on the WAM-Sahel rainfall; implying that the monsoon system becomes more active and precipitation increases (as in observational Fig. 15-right). It is also important to notice the absence of an anomalous state in both the TEJ and AEJ, suggesting its weak role over Sahel.

## Future collaboration with host institution

Further work to develop with Met Office-Hadley Centre includes:

- Move the 'RWS_diagnostic' script from PV-Wave (current software) on Interface Definition Language (IDL) programming language (future software)

- Make a profound assessment of deficiencies and uncertainties in the Mediterranean link to WAM-Sahel monsoon in HadGEMs coupled models; for a future report and looking towards improving the HadGEM3-model development

- Use the Extended-MCA technique in the post-processing of seasonal forecasts; it could produce a significant increase in skill

- Study with coupled experiments of the potential connection between the Mediterranean Sea and the Pacific Decadal Oscillation after analysing the EMCA-based sensitivity experiment performed with UCLA-AGCM

Additionally, in the Appendix, I am attaching a letter of introduction from Alberto Arribas, tutor of my exchange-visit at Met Office.

## Projected publications/articles resulting or to result from your grant

We are preparing two publications:

"Large-scale atmospheric response to Mediterranean summer SST anomalies" (ready for submitting to *Climate Dynamics*); showing the observational evidence and testing the hypothesis with AGCM large-simulation.

"Recent impacts of Mediterranean SSTs on West African rainfall variability" (in elaboration for submission). In this paper, Med-EMCA results based on observations and a large-run simulation with the UCLA-AGCM model, at the expense of analysis from the model-sensitivity experiment, are described in relation to the WAM system.

## Comments

I thank Jucundus Jacobeit and Laurent Li for their constructive comments on the preliminary study presented in the 2nd ESF-MedCLIVAR Workshop.

I would also like to thank, from Hadley Centre, Stephen Cusack, Adam Scaife, Matthew Collins, Sarah Ineson, Margaret Gordon and Drew Peterson for useful discussions and comments regarding this study. Thanks are also due to Ian Culverwell for his constant help and assistance in pp_routines for computing streamfunction and velocity potential.

I wish to thank Teresa Losada and Irene Polo, at UCM, for technical support and valuable advice on implementation and use of HadGEMs model-data in GrADS and Matlab softwares. I would also like to thank Ellen Degott, from the ESF Office, for her patience and encouragement.

Finally, I would like to express my gratitude to ESF-MedCLIVAR Programme for making this exchange-visit possible. As proof of this fruitful work, apart from possible publications, I have given a seminar concerning the study carried out in the Department of Geophysics and Meteorology in my Faculty (at UCM); I enclose the announcement in the Appendix.

In addition, the reflection about this grant makes me indicate that the visit to a host institution, particularly in the Hadley Centre with its awesome environment, generates so amount of insightful discussions that helps to fall on a great number of different and enriching points of view concerning the study. Really, it was a very pleasant time for me, although I think that it was not time enough to get used to completely working on the host daily-routine.

## References

Barnett, T. P., D. W. Pierce, M. Latif, D. Dommenget, and R. Saravanan (1999): Interdecadal interactions between the tropics and midlatitudes in the Pacific basin. *Geophys. Res. Lett.*, **26**: 615-618.

Berry, G. J., and C. D. Thorncroft (2005): Case study of an intense African easterly wave. *Mon. Wea. Rev.,* **133,** 752–766.

Biasutti, M and Giannini, A. (2006): Robust Sahel drying in response to late 20th century focings. *Geophys. Res. Lett.*, **33**, doi:10.1029/2006GL026067.

Bladé, I. (1997): The influence of midlatitude ocean–atmosphere coupling on the low-frequency variability of a GCM. Part I: No tropical SST forcing. *J. Climate,* **10,** 2087–2106.

Bond, N.A. and D.E. Harrison (2000): The Pacific Decadal Oscillation, air-sea interaction and central north Pacific winter atmospheric regimes. *Geophys. Res. Lett.*, **27**(5), 731-734.

Branstator, G. (2002): Circumglobal teleconnections, the jet stream waveguide, and the North Atlantic Oscillation. *J. Climate*, **15**, 1893–1910.

Bretherton, S. B., C. Smith, and J. H. Wallace (1992): An intercomparation of methods for finding coupled patterns in climate data, *J. Climate,* **5***,* 541-560.

Cane, M. A., Clement, A. C., Kaplan, A., Kushnir, Y., Pozdnyakov, D., Seager, R., Zebiak, S. E. and Murtugudde, R. (1997): Twentieth- Century Sea Surface Temperature trends. *Science* **275**, 957–960, DOI: 10.1126/science.275.5302.957.

Chang, E. K., S. Lee and K. L. Swanson (2002): Storm track dynamics. *J. Climate*, **15**, 2163-2183.

Cook, K.H. (1999): Generation of the African Easterly Jet and Its Role in Determining West African Precipitation. *J. Climate*, **12**, 1165–1184

Czaja, A. and C. Frankignoul (2002): Observed impact of Atlantic SST anomalies on the North Atlantic Oscillation. *J. Climate*, **15**, 606-623.

Ding, Q. and B. Wang (2005): Circumglobal teleconnections in the Northern Hemisphere summer. *J. Climate*, **18**, 3483-3505.

Douville, H., S. Conil, S. Tyteca and A. Voldoire (2007): Soil moisture memory and West African monsoon predictability: artefact or reality?. *Climate Dyn.*, **28**, 723-742.

Fontaine, B., P. Roucou, and S. Trzaska, 2003: Atmospheric water cycle and moisture fluxes in the West African monsoon: mean annual cycles and relationship using NCEP/NCAR reanalyses, *Geophys. Res. Lett.,* **30**, 10.1029-10.1032.

Fontaine B., P. Roucou and S. Sivarajan (2008): The relationship between surface temperatures over the Mediterranean and West African monsoon. Part I: observed connection patterns (1979-2006). *J. Geophys. Res*. Submitted.

Frankignoul C., A. Czaja and B. L'Heveder (1998): Air–Sea Feedback in the North Atlantic and Surface Boundary Conditions for Ocean Models. *J. Climate*, **11**, 2310-2324.

Frankignoul, C. and E. Kestenare (2005): Observed Atlantic SST anomaly impact on the NAO: An update. *J. Climate*, **18**, 4089-4094.

García-Serrano, J., I. Polo, B. Rodríguez-Fonseca and T. Losada (2007): Summer-fall tropical precipitation related to Mediterranean SST anomalies. Poster presentation at 2nd ESF MedCLIVAR Workshop.

García-Serrano J., T. Losada, B. Rodríguez-Fonseca and I. Polo (2008): Tropical Atlantic Variability modes (1979-2002). Part II: time-evolving atmospheric circulation related to SST-forced tropical convection. *J. Climate*. DOI: 10.1175/2008JCLI2191.1

Gershunov, A. and T. P. Barnett (1998): Interdecadal modulation of ENSO teleconnections. *Bull. Amer. Meteor. Soc.*, **79**, 2715-2725.

Giannini, A., R. Saravanan and P. Chang (2003): Oceanic Forcing of Sahel Rainfall on Interannual to Interdecadal Time Scales. *Science.*, **302**, 1027–1030.

Grist, J. P., S. E. Nicholson and A. I. Barcilon (2002): Easterly Waves over Africa. Part II: Observed and Modeled Contrasts between Wet and Dry Years. *Mon. Wea. Rev.,* **130**, 212-225.

Haarsma R., F. Selten, N. Weber and M. Kliphuis (2008): Sahel Rainfall variability and response to Greenhouse Warming. *Geophys. Res. Lett.* (submitted).

Hall, N. M. J., G. Kiladis, and C. Thorncroft (2006): Threedimensional structure and dynamics of African easterly waves. Part II: Dynamical modes. *J. Atmos. Sci.,* **63,** 2231–2245.

Held, I. M., T. L. Delworth, J. Lu, K. L. Findell, and T. R. Knutson (2005): Simulation of Sahel drought in the 20th and 21st centuries. *Proc. Natl. Acad. Sci.*, **102**, 17.891–17.896.

Hoerling M, Hurrell J, Eischeid J, Phillips A (2006): Detection and Attribution of Twentieth-Century Northern and Southern African Rainfall Change. *J Climate*, **19**, 3989–4008.

Hoskins, B. J., I. N. James and G. H. White, 1983: The shape, prop agation, and mean-flow interaction of large-scale weather sys tems. *J. Atrnos. Sci.*, **40**, 1595-1612.

Hoskins, B. J. and T. Ambrizzi (1993): Rossby wave propagation on a realistic longitudinally varying flow. *J. Atmos. Sci.*, **50**, 1661-1671.

Hsieh, J.-S. and K. H. Cook (2005): Generation of African Easterly disturbances: relationship to the African Easterly jet. *Mon. Wea. Rev.,* **133**, 1311-1327.

Janicot S.and B. Sultan (2001): Intra-seasonal modulation of convection in the West African monsoon. *Geophys. Res. Lett*., **28**, 523-526.

Janicot, S., A. Harzallah, B. Fontaine and V. Moron (1998): West African Monsoon Dynamics and Eastern Equatorial Atlantic and Pacific SSTAnomalies(1970–88). *J. Climate*, **11**,1874-1882.

Joly M., A. Voldoire, H. Douville, P. Terray, and J.-F. Royer (2007): African monsoon teleconnections with tropical SSTs: validation and evolution in a set of IPCC4 simulations. *Clim. Dyn*., **29**, 1-20. doi: 10.1007/s00382-006-0215-8.

Jung, T., L. Ferranti, and A. M. Tompkins (2006): Response to the summer of 2003 Mediterranean SST anomalies over Europe and Africa, *J. Climate,* **19***,* 5439–5454.

Kodera, K., and Y. Kuroda (2003): Regional and hemispheric circulation patterns in the northern hemisphere winter, or the NAO and the AO. *Geophys. Res. Lett.*, doi:10.1029/2003GL017290.

Kundu, P.K. (1990): *Fluid Mechanics*. Academic Press, Inc., 638 pp.

Li LZX (2006): Atmospheric GCM response to an idealized anomaly of the Mediterranean sea surface temperature. *Clim Dyn*, **27**, 543-552.

Matthews, A. J. and G. N. Kiladis (1999a): The Tropical–Extratropical Interaction between High-Frequency Transients and the Madden–Julian Oscillation. *Mon. Wea. Rev.,* **127**, 661-677.

Matthews, A. J. and G. N. Kiladis (1999b): Interactions between ENSO, Transient Circulation, and Tropical Convection over the Pacific. *J. Climate,* **12**, 3062-3086.

Mechoso, C. R., J.-Y. Yu and A. Arakawa (2000): A coupled GCM pilgrimage: from climate catastrophe to ENSO simulations. Proceeding of a Symposium in Honor of Prof. Akia Arakawa. Editor D.A. Randall, 539-575.

Mekonnen, A., C. D. Thorncroft and A. R. Aiyyer (2006): Analysis of Convection and Its Association with African Easterly Waves. *J. Climate*, **19**, 5405-5421.

Michaelides, Silas Chr, (1983): Components of large-scale kinetic energy generation during an eastern Mediterranean cyclogenesis. *Meteor. and Atmosp. Physics*, **32**, 247-256.

Mohíno, E., B. Rodríguez-Fonseca, S. Gervois, S. Janicot, T. Losada, J. Bader, P. Ruti (2008): SST-forced signals on West African rainfall from AGCM simulations-PartI: Intercomparison of models. *Clim. Dyn.*, submitted

Moron V., N. Philippon and B. Fontaine (2004): Simulation of West African monsoon circulation in four atmospheric general circulation models forced by prescribed sea surface temperature. *J. Geophys. Res.*, **109**, doi:10.1029/2004JD004760.

Nicholson, S. E. (2008): The intensity, location and structure of the tropical rainbelt over west Africa as factors in interannual variability. *Int. J. Climatol..,* DOI: 10.1002/joc.1507.

Nicholson, S. E. and J. P. Grist (2001) : A conceptual model for understanding rainfall variability in the West African Sahel on interannual and interdecadal timescales. *Int*. *J*. *Climatol*. **21**, 1733–1757.

Nicholson, S. E., A. I. Barcilon, M. Challa and J. Baum (2007): Wave Activity on the Tropical Easterly Jet. *J. Climate*, **64**, 2756-2763.

Nicholson, S. E., A. I. Barcilon and M. Challa (2008): An Analysis of West African Dynamics Using a Linearized GCM. *J. Atm. Sci.*, **65**, 1182-1203.

Okumura, Y. and S.-P. Xie (2004): Interaction of the Atlantic Equatorial Cold Tongue and the African Monsoon. *J. Climate,* **17**, 3589–3602.

Polo I., B. Rodríguez-Fonseca, T. Losada and J. García-Serrano (2008): Tropical Atlantic Variability modes (1979-2002). Part I: time-evolving SST modes related to West African rainfall. *J. Climate*, DOI: 10.1175/2008JCLI2607.1 (in press).

Qin, J. and W. A. Robinson, 1993: On the Rossby wave source and the steady linear response to tropical forcing. *J. Atmos. Sci.*, **50**, 1819-1823.

Raicich, F., N. Pinardi and A. Navarra (2003): Teleconnections between Indian monsoon and Sahel rainfall and the Mediterranean. *Int. J. Climatol.* **23**, 173–186.

Renwick, J. A. and M. J. Revell (1999): Blocking over the South Pacific and Rossby Wave Propagation. *Mon. Wea. Rev.,* **127**, 2233-2247.

Rodwell, M. J. and B. Hoskins (1996): Monsoons and the dynamics of deserts. *Q. J. R. Meteorol. Soc.*, **122**, 1385-1404.

Rowell, D. P. (2001): Teleconnections between the tropical Pacific and the Sahel. *Q. J. R. Meteorol. Soc.*, **127**, 1683-1706.
Rowell, D. P. (2003): The impact of the Mediterranean SSTs on the Sahelian rainfall season. *J. Climate*, **16**, 849-862.

Sardeshmukh, P. D. and B. Hoskins (1987): On the derivation of the divergent flow from the rotational flow: the chi problem. *Q. J. R. Meteorol. Soc.*, **113**, 339-360.

Seidel, D. J., Fu, Q., Randel, W. J. and Reichler, T. J. (2008): Widening of the tropical belt in a changing climate. *Nature geoscience* **1**, 21-24, doi:10.1038/ngeo.2007.38.

Sultan, B. and S. Janicot (2000): Abrupt shift of the ITCZ over West Africa and intra-seasonal variability. *Geophys. Res. Lett.*, **27**, 3353-3356.

Trenberth, K. E. (1986): An assessment of the impact of transient eddies on the zonal flow during a blocking episode using localized Eliassen–Palm flux diagnostics. *J. Atmos. Sci.,* **43,** 2070–2087.

Trenberth, K.E. and J.W. Hurrell (1994): Decadal atmosphere-ocean variations in the Pacific. *Clim. Dyn.*, **9**, 303-319.

Wallace, J. M., G.H. Lim and M. L. Blackmon (1988): Relationship between cyclone tracks, anticyclone tracks, and baroclinic waveguides. *J. Atmos. Sci.*, **45**, 439-462.

Wang, C. (2002): Atlantic Climate Variability and Its Associated Atmospheric Circulation Cells. J. Climate, 15, 1516-1536.

Watanabe, M. (2004): Asian Jet Waveguide and a Downstream Extension of the North Atlantic Oscillation. *J. Climate*, **17**, 4674-4691.

Xoplaki, E., J.F. González-Rouco, D. Gyalistras, J. Luterbacher, R. Rickli and H. Wanner (2003a): Interannual summer air temperature variability over Greece and its connection to the large-scale atmospheric circulation and Mediterranean SSTs 1950-1999. *Clim. Dyn.*, **20**, 537-554.

Xoplaki, E., J.F. González-Rouco, J. Luterbacher and H. Wanner (2003b): Mediterranean summer air temperature variability and its connection to the large-scale atmospheric circulation and SSTs. *Clim. Dyn.*, **20**, 723-739.

Zhang, Y., J.M. Wallace and D.S. Battisti (1997): ENSO-like interdecadal variability: 1900-93. *J. Climate*, **10**, 1004-1020.